



THE UNIVERSITY *of* EDINBURGH

Edinburgh Research Explorer

A solid-phase combinatorial approach for indoloquinolizidine-peptides with high affinity at D1 and D2 dopamine receptors

Citation for published version:

Molero, A, Vendrell, M, Bonaventura, J, Zachmann, J, Lopez, L, Pardo, L, Lluís, C, Cortes, A, Albericio, F, Casado, V & Royo, M 2015, 'A solid-phase combinatorial approach for indoloquinolizidine-peptides with high affinity at D1 and D2 dopamine receptors', *European Journal of Medicinal Chemistry*, vol. 97, pp. 173–180. <https://doi.org/10.1016/j.ejmech.2015.04.052>

Digital Object Identifier (DOI):

[10.1016/j.ejmech.2015.04.052](https://doi.org/10.1016/j.ejmech.2015.04.052)

Link:

[Link to publication record in Edinburgh Research Explorer](#)

Document Version:

Peer reviewed version

Published In:

European Journal of Medicinal Chemistry

General rights

Copyright for the publications made accessible via the Edinburgh Research Explorer is retained by the author(s) and / or other copyright owners and it is a condition of accessing these publications that users recognise and abide by the legal requirements associated with these rights.

Take down policy

The University of Edinburgh has made every reasonable effort to ensure that Edinburgh Research Explorer content complies with UK legislation. If you believe that the public display of this file breaches copyright please contact openaccess@ed.ac.uk providing details, and we will remove access to the work immediately and investigate your claim.



Accepted Manuscript

A Solid-Phase Combinatorial Approach for Indoloquinolizidine-Peptides with High Affinity at D₁ and D₂ Dopamine Receptors

Anabel Molero, Marc Vendrell, Jordi Bonaventura, Julian Zachmann, Laura López, Leonardo Pardo, Carme Lluís, Antoni Cortés, Fernando Albericio, Vicent Casadó, Miriam Royo

PII: S0223-5234(15)30015-5

DOI: [10.1016/j.ejmech.2015.04.052](https://doi.org/10.1016/j.ejmech.2015.04.052)

Reference: EJMECH 7867

To appear in: *European Journal of Medicinal Chemistry*

Received Date: 21 November 2014

Revised Date: 18 April 2015

Accepted Date: 25 April 2015

Please cite this article as: A. Molero, M. Vendrell, J. Bonaventura, J. Zachmann, L. López, L. Pardo, C. Lluís, A. Cortés, F. Albericio, V. Casadó, M. Royo, A Solid-Phase Combinatorial Approach for Indoloquinolizidine-Peptides with High Affinity at D₁ and D₂ Dopamine Receptors, *European Journal of Medicinal Chemistry* (2015), doi: 10.1016/j.ejmech.2015.04.052.

This is a PDF file of an unedited manuscript that has been accepted for publication. As a service to our customers we are providing this early version of the manuscript. The manuscript will undergo copyediting, typesetting, and review of the resulting proof before it is published in its final form. Please note that during the production process errors may be discovered which could affect the content, and all legal disclaimers that apply to the journal pertain.



A Solid-Phase Combinatorial Approach for Indoloquinolizidine-Peptides with High Affinity at D₁ and D₂ Dopamine Receptors

Anabel Molero,^{†‡} Marc Vendrell,^{†‡*} Jordi Bonaventura,[§] Julian Zachmann,^{††} Laura López,^{††} Leonardo Pardo,^{††} Carme Lluís,[§] Antoni Cortés,[§] Fernando Albericio,^{‖¶} Vicent Casadó,[§] and Miriam Royo^{†¶*}

RECEIVED DATE (to be automatically inserted after your manuscript is accepted if required according to the journal that you are submitting your paper to)

[†] Combinatorial Chemistry Unit, Barcelona Science Park, University of Barcelona, 08028 Barcelona, Spain.

[‡] MRC Centre for Inflammation Research, Queen's Medical Research Institute, University of Edinburgh, EH16 4TJ Edinburgh, United Kingdom.

[§] Centro de Investigación Biomédica en Red sobre Enfermedades Neurodegenerativas. (CIBERNED) and Department of Biochemistry and Molecular Biology, Faculty of Biology, University of Barcelona, 08028 Barcelona, Spain.

^{††} Laboratori de Medicina Computacional, Unitat de Bioestadística, Facultat de Medicina, Universitat Autònoma de Barcelona, 08193 Bellaterra, Spain.

[¶] CIBER-BBN, Networking Centre on Bioengineering, Biomaterials and Nanomedicine, Barcelona Science Park, 08028 Barcelona, Spain.

[‖] Institute for Research in Biomedicine, 08028 Barcelona, Spain.

[‡] Current address: International Maize and Wheat Improvement Center (CIMMYT), Mexico City, 06 600, Mexico.

* To whom correspondence should be addressed. Phone: +34 934037122, e-mail: mroyo@pcb.ub.cat; Phone : +44 1312426685, e-mail: mvendrel@staffmail.ed.ac.uk.

Abstract.

Ligands acting at multiple dopamine receptors hold potential as therapeutic agents for a number of neurodegenerative disorders. Specifically, compounds able to bind at D₁R and D₂R with high affinity could restore the effects of dopamine depletion and enhance motor activation on degenerated nigrostriatal dopaminergic systems. We have directed our research towards the synthesis and characterisation of heterocycle-peptide hybrids based on the indolo[2,3-*a*]quinolizidine core. This privileged structure is a water-soluble and synthetically accessible scaffold with affinity for diverse GPCRs. Herein we have prepared a solid-phase combinatorial library of 80 indoloquinolizidine-peptides to identify compounds with enhanced binding affinity at D₂R, a receptor that is crucial to re-establish activity on dopamine-depleted degenerated GABAergic neurons. We applied computational tools and high-throughput screening assays to identify **9a{1,3,3}** as a ligand for dopamine receptors with nanomolar affinity and agonist activity at D₂R. Our results validate the application of indoloquinolizidine-peptide combinatorial libraries to fine-tune the pharmacological profiles of multiple ligands at D₁ and D₂ dopamine receptors.

Keywords: privileged scaffolds, solid-phase synthesis, GPCRs, neurodegenerative diseases, heterocycles.

Introduction.

The solid-phase synthesis of combinatorial libraries and their screening has proven effective for the identification of bioactive compounds and their subsequent optimisation, especially when the synthetic routes have sufficient generality to produce novel analogues of interest.¹⁻⁶ We have directed our research towards privileged scaffolds as templates for biologically active molecules at multiple therapeutic targets, and described the synthesis and characterisation of heterocycle-peptide hybrids as ligands for G-protein coupled receptors (GPCRs).^{7,8} Among GPCRs, structures simultaneously binding at multiple dopamine receptor subtypes hold potential as therapeutic agents for the treatment of neurodegenerative disorders, such as Parkinson's disease (PD).^{9,10} Dual molecules with ability to bind both dopamine D₁R and D₂R could restore the effects of dopamine depletion and enhance motor activation on degenerated nigrostriatal dopaminergic systems via simultaneous activation of the direct pathway (i.e. via D₁R on striatonigral neurons) and repression of the inhibitory indirect pathway (i.e. via D₂R on striatopallidal GABAergic neurons).¹¹ Our group has reported the preparation of ergolene-peptide^{12,13} and indolo[2,3-*a*]quinolizidine-peptide hybrids as ligands for dopamine receptors.^{14,15} The indolo[2,3-*a*]quinolizidine structure is a water-soluble and synthetically accessible scaffold resembling indoloazecine and tetrahydro- β -carboline systems with affinity for a number of GPCRs.¹⁶ Our first studies with indoloquinolizidine-peptides identified a number of compounds with medium to high affinity for D₁R and D₂R. While those compounds presented submicromolar affinity at D₁R, their affinities at D₂R were limited to the low micromolar range. Herein we have designed a solid-phase combinatorial library of 80 new indoloquinolizidine-peptide hybrids to enhance their binding affinity at D₂R, a receptor that is crucial to re-establish activity on dopamine-depleted degenerated GABAergic neurons, that could lead to potential dual ligands for D₁R and D₂R. We have screened our library using radioligand binding and ERK1/2 phosphorylation assays

to identify new indoloquinolizidine-peptides maintaining high affinities at D₁R while achieving enhanced nanomolar binding affinity and agonist activity at D₂R.

Results and Discussion.

Library design. Indolo[2,3-*a*]quinolizidines are excellent structures for combinatorial medicinal chemistry because of their straightforward synthesis and diverse pharmacological properties. We previously optimised the synthesis of indolo[2,3-*a*]quinolizidine carboxylic acids based on the protocol of Wenkert *et al.* (acid cyclization of *N*-tryptophyl-1,4-dihydropyridines to afford indoloquinolizidines).¹⁷ Both *cis* (**1**) and *trans* (**2**) diastereoisomers (Figure 1a) are racemic compounds and can be prepared in multigram scale with high purities after five synthetic steps. In order to facilitate the preparation of combinatorial libraries of indoloquinolizidine-peptides (**3**, Figure 1b), we optimised the incorporation of **1** and **2** to solid-phase peptide synthesis (SPPS). To the best of our knowledge, our approach represents the first adaptation of indolo[2,3-*a*]quinolizidines to solid-phase chemistry. We prepared indoloquinolizidine-peptides with variable stereochemistry at C₃ and C_{12b} of the indolo[2,3-*a*]quinolizidine core and different tripeptides for enhanced affinity at D₁R and D₂R. Previous studies with indoloquinolizidine-peptides indicated the heterocyclic core as the major responsible for the interaction at the binding sites while tripeptides mainly interacted with the extracellular regions of dopamine receptors. In the present work, we explored different peptides around the indoloquinolizidine core to increase the binding affinity at D₂R and generate multiple D₁/D₂ high-affinity ligands.

Figure 1. a) Building blocks employed in the synthesis of the library; b) general structure of indoloquinolizidine-peptides.

We have designed a library of novel indoloquinolizidine-tripeptides using combinations of 9 different amino acids. As *C*-terminal amino acids (AA3, Figure 1a), we employed neutral and positively-charged cyclic amino acids (i.e. Pro and Amp) as well as one linear positively-charged amino acid (Lys). This selection was based on the electrostatic nature of the extracellular surface of dopamine receptors. As shown in the molecular electrostatic potential of D₂R from the extracellular side (Figure 2), E95^{2,65} in TM2 (Ballesteros & Weinstein numbering scheme¹⁸ is shown as superscript) and E181ⁱ⁻¹ in ECL2 (at position *i*-1 relative to the conserved C180ⁱ engaged in a disulfide bond with C107^{3,25} in TM3) confer a negative character to the channel linking the extracellular environment and the binding site cavity. Therefore, we envisaged that a positive charge at the *C*-terminal position may favour an ionic interaction with the extracellular region and enhance binding affinity at D₂R. For the central position of the tripeptide (AA2, Figure 1a) we selected four different aromatic amino acids (Phe(4-F), Phe(3,4-F₂), Trp and Tyr) to explore the influence of H-bond donor and acceptor groups (e.g. Trp as a non-polar aromatic H-bond donor, Tyr as a polar aromatic H-bond donor and acceptor) as well as hydrophobic fluorinated amino acids, which were well tolerated in previous heterocycle-peptide hybrid libraries.¹³ Finally, we incorporated four diverse amino acids (e.g. cyclic (Pro), linear and hydrophobic (Nle), positively (Lys) and negatively-charged (Glu)) to explore a relatively broad chemical space at the *N*-terminal position of the tripeptide attached to the alkaloid (AA1, Figure 1a). Notably, all peptide combinations were prepared with and without an aminohexanoic spacer to assess the interaction of the tripeptides at different extracellular regions of D₁R and D₂R. We limited the size of the library to 80 indoloquinolizidine-peptides with 20 different peptide combinations, which did not repeat any amino acid and did not contain more than one positive charge.

Figure 2. Illustration of the molecular electrostatic potential at the extracellular surface of D₂R.

Chemical synthesis. Since there are no reports of indolo[2,3-*a*]quinolizidines being loaded and released from polystyrene (PS) solid supports, we optimised the coupling and cleavage conditions of **1** and **2** onto Rink-MBHA-PS as well as on two PS-supported tripeptides (i.e. Glu-Trp-Pro-Rink-MBHA-PS and Pro-Tyr-Lys-Rink-MBHA-PS). Couplings using PyBOP and HOAt in the presence of DIPEA yielded the corresponding amides in high purities within 2 h (Table 1). To examine whether **1** and **2** were stable under conventional cleavage conditions and there was no epimerization of the C_{12b} of the indolo[2,3-*a*]quinolizidine core,^{19,20} we treated both diastereoisomers with TFA:H₂O:DCM (95:2.5:2.5) and confirmed by HPLC that the indolo[2,3-*a*]quinolizidine core was unaffected after treatment with high concentrations of trifluoroacetic acid (TFA) (Figure S1 in Electronic Supporting Information (ESI)).

Table 1.

After preparing all 20 tripeptides using standard SPPS conditions (DIC and HOBt as an additive, Scheme 1), the resulting chemset **4** was split into two aliquots, one of which was modified with Fmoc-amino hexanoic acid to render the chemset **5**. Carboxylic acids **1** and **2** were attached to both chemsets **4** and **5** using the above mentioned conditions (Scheme 1). The cleavage of the library was performed using optimised conditions for compounds with positively-charged C-terminal amino acids (TFA:H₂O:DCM, 30:5:65)²¹ and TFA:H₂O:DCM (95:2.5:2.5) for the rest of the library. The final 80 indoloquinolizidine-peptides were isolated in very high purities (> 90%) after simple solid-phase extraction or semi-preparative RP-HPLC. All 80 compounds were characterised by HPLC-MS prior to the biological assays (Tables S1 and S2 in ESI).

Scheme 1. Solid-phase synthesis of a combinatorial library of indoloquinolizidine-peptides. Reaction conditions: a) Fmoc-AA₃-OH, DIC, HOBT, b) piperidine-DMF (2:8), c) Fmoc-AA₂-OH, DIC, HOBT, d) Fmoc-AA₁-OH, DIC, HOBT, e) Fmoc-Ahx-OH, DIC, HOBT, f) **1**, PyBOP, HOAt, DIPEA, g) TFA:H₂O:DCM, h) **2**, PyBOP, HOAt, DIPEA.

Binding assays and structure-affinity relationships. The binding affinities of indoloquinolizidine-peptides for D₁R and D₂R were examined by competitive radioligand displacement against the D₁R antagonist [³H]-SCH 23390 and the D₂R antagonist [³H]-YM 09151-2, respectively, in membrane preparations from sheep striatum. Weak binding was observed in compounds containing negatively charged amino acids (i.e. Glu) in the tripeptide moiety, whereas binding affinities were significantly increased when a positively charged amino acid (e.g. Lys, Arg) was included at the C-terminal position (Figure S2 in ESI). This observation confirmed our hypothesis that positively charged residues may enhance binding affinity by interacting with the anionic extracellular regions of dopamine receptors. From our primary screen we also observed some preference in the stereochemistry of the indoloquinolizidine scaffold, especially at D₂R. *Cis* derivatives showed low to moderate affinities at D₂R while stronger interactions were obtained for the corresponding *trans* derivatives. The incorporation of the aminohexanoic spacer at D₂R had variable results: in some compounds the spacer slightly improved the affinity at D₂R (e.g. **7**{3,1,1} vs. **9**{3,1,1} or **7**{3,2,1} vs. **9**{3,2,1}), while in some others binding affinities remained unaffected (e.g. **7**{2,4,2} vs. **9**{2,4,2} or **7**{4,2,1} vs. **9**{4,2,1}) (Figure S2 in ESI).

A group of 10 indoloquinolizidine-peptides with the best binding profiles at D₁R and D₂R (e.g. **9**{2,2,2}, **9**{2,4,2}, **7**{2,1,3}, **9**{1,2,3}, **7**{2,2,3}, **9**{1,3,3}, **7**{2,3,3}, **9**{2,4,3}, **6**{2,4,2}, **8**{2,1,3}) was further examined and their affinity constants (*K_D*) were determined. Most of the selected indoloquinolizidine-peptides showed monophasic competition curves at D₁R (i.e.

no distinction between high and low-affinity states), thus we compared their K_D average values at D_1R . On the other hand, when competition curves at D_2R were biphasic, we determined both their high-affinity (K_{D1}) and low-affinity (K_{D2}) constants.

Table 2.

Notably, compounds consisting of the same tripeptide and *trans* indoloquinolizidine - regardless of the presence/absence of aminohexanoic spacer- showed remarkably lower K_D values at D_2R than the corresponding *cis* derivatives, which corroborates the importance of the indoloquinolizidine stereochemistry for the interaction at dopamine receptors. Specifically, we compared **9{2,4,2}** and **6{2,4,2}** as two indoloquinolizidine-peptides with the same tripeptide (i.e. Nle-Phe(4F)-Amp) and different indoloquinolizidine configuration (i.e. *trans* for **9{2,4,2}** and *cis* for **6{2,4,2}**). As shown in Table 2, the K_{D1} for **9{2,4,2}** at D_2R was 10 times lower than the one for **6{2,4,2}**, proving the higher affinity of the *trans* compound at D_2R . This observation was also corroborated for the derivatives **7{2,1,3}** and **8{2,1,3}**, which contained the same tripeptide (i.e. Nle-Tyr-Lys). In this case, the *trans* derivative **7{2,1,3}** showed a K_{D1} at D_2R around 1.5 times lower than the *cis* derivative **8{2,1,3}**. In addition to showing affinities in the submicromolar range at D_1R and nanomolar range at D_2R , selected indoloquinolizidine-peptides showed marginal binding (medium and high micromolar range) at other GPCRs in brain striatum (e.g. adenosine A_1 and A_{2A} receptors, Table S3 in ESI). We selected **9{1,3,3}** as a multiple ligand for dopamine receptors with some D_2R selectivity, showing micromolar affinity at D_1R and nanomolar affinity at D_2R . Molecules with such pharmacological profile are excellent candidates to restore the effects of dopamine depletion and enhance motor activation without causing any dysregulation of the trafficking and desensitization of D_1R , which could lead to undesired dyskinesias.^{22,23} Furthermore, the scale-up synthesis of **9{1,3,3}** enabled the isolation of the two *trans* diastereoisomers that were characterised and named as **9a{1,3,3}** and **9b{1,3,3}** (Figure 3).

Figure 3. Chemical structures of isolated *trans* diastereoisomers of **9{1,3,3}**.

We measured the high-affinity (K_{D1}) and low-affinity (K_{D2}) constants for **9a{1,3,3}** and **9b{1,3,3}** at D_1R and D_2R in membrane preparations from sheep striatum by competition assays, where constant concentrations of D_1R and D_2R antagonists ($[^3H]$ -SCH 23390 and $[^3H]$ -YM 09151-2, respectively) were co-incubated with increasing concentrations of **9a{1,3,3}** and **9b{1,3,3}** (Figure S3 in ESI). Notably, the two diastereoisomers showed biphasic competition curves at D_1R and D_2R , and we determined both their K_{D1} and K_{D2} constants at the two receptors (Table 3). The different stereochemistry of the two indoloquinolizidine-peptides led to significantly higher affinity of **9a{1,3,3}** at the D_2R low-affinity state (K_{D2}), whereas no significant differences were detected between the binding values of **9a{1,3,3}** and **9b{1,3,3}** at any of the affinity states of D_1R (Table 3). These results correlated with our *in silico* assays at D_2R (Figure 4), and allowed us to assign the absolute stereochemistry of **9a{1,3,3}** as the diastereoisomer with the best molecular fitting at this receptor. Altogether, this data confirmed our previous observation that binding at D_2R shows higher dependency on the stereogenicity of the indoloquinolizidine core, while affinities at D_1R are not largely affected by the stereochemistry of the indoloquinolizidine structure.

Table 3.

Encouraged by the high binding affinity of **9a{1,3,3}** at D_2R , we examined its behavior at the receptor. We assessed whether **9a{1,3,3}** could bind allosterically at D_2R since indoloquinolizidine derivatives have been described as allosteric ligands for dopamine receptors.¹⁴ We performed dissociation kinetic assays in membranes that were pre-incubated with or without **9a{1,3,3}** before adding different concentrations of the orthosteric radioligand $[^3H]$ -YM 09151-2. After 2 h the dissociation was initiated by addition of YM 09151-2 and we measured the total binding at every time point by rapid filtration and

radioactivity counting. As shown in Table 4, the addition of **9a{1,3,3}** did not significantly alter the K_{off} of YM 09151-2 at D₂R, which suggests that **9a{1,3,3}** does not behave as an allosteric modulator at D₂R.

Table 4.

Computational model of D₂R in complex with 9a{1,3,3}. In an attempt to get a better understanding of the interaction between indoloquinolizidine-peptides and D₂R, we constructed a three-dimensional model of the complex between **9a{1,3,3}** and a homology model of D₂R. The indoloquinolizidine moiety of the ligand was docked into the orthosteric binding pocket of the receptor in such a manner that the protonated NH group of the ring formed an ionic interaction with D114^{3,32} and the indole part formed edge-to-face aromatic-aromatic interactions with W386^{6,48} and F390^{6,52} (Figure 4a). The aminohexanoic spacer expanded through a channel located between the extracellular segments of TMs 2, 3 and 7 towards the extracellular environment, which has been proposed to be part of the ligand entry/exit pathway to/from the orthosteric binding site.²⁴ We refined this initial binding mode using molecular dynamics (MD) simulations of the ligand-receptor complex (see Experimental section). The structures of the ligand-receptor complex computed during MD simulations are depicted in Figure 4b. Importantly, the key proposed interactions between the indoloquinolizidine moiety of **9a{1,3,3}** and the orthosteric binding cavity of the receptor remained stable through the simulation time. The tripeptide moiety of **9a{1,3,3}** expanded towards the extracellular part so that lysine could form an ionic interaction with E95^{2,65} in TM2. It is important to note that other initial docking poses in which lysine was placed in close proximity to E181ⁱ⁻¹ modified its conformation during the simulation time to finally accomplish the interaction with E95^{2,65}. Furthermore, the aromatic ring of the central position of the tripeptide formed aromatic-aromatic interactions with Y408^{7,35}, the fluorine atoms formed halogen bonds with N396^{6,58} and the terminal acetamide group acted as both

hydrogen bond donor and acceptor with the backbone C=O and N-H groups of C180ⁱ in ECL2.

Figure 4. Molecular dynamics simulations of D₂R in complex with 9a{1,3,3}. a) The structure of the ligand-receptor complex computed during MD trajectories. 9a{1,3,3} is shown in white and the side chains of D₂R are shown in green; b) detailed view of the interactions between 9a{1,3,3} and D₂R.

Functional assays. We further examined the agonist/antagonist behaviour of 9a{1,3,3} at D₂R by evaluating the MAPK signal transduction pathway in CHO cells that were transfected with D₂R. As shown in

Figure 5, 9a{1,3,3} increased the ERK1/2 phosphorylation in a dose-dependent manner, similar to the D₂R agonist quinpirole (QP). This result confirms that 9a{1,3,3} behaves as an agonist at D₂R. Furthermore, combined administration of YM 09151-2, an antagonist of D₂R, and 9a{1,3,3} did not diminish the capacity of YM 09151-2 to decrease ERK1/2 phosphorylation, thereby indicating that the 9a{1,3,3} does not behave as a D₂R antagonist.

Figure 5. Functional characterisation of 9a{1,3,3} at D₂R. CHO cells expressing D₂R were cultured in serum-free medium for 16 h prior to the addition of any ligand. Cells were treated (or not) with 1 μM YM 09151-2. After 5 min, 1 μM quinpirole (QP), increasing concentrations of compound 9a{1,3,3} or combined 10 μM 9a{1,3,3} with YM 09151-2 were incubated for further 5 min and the extent of ERK1/2 phosphorylation was determined as described in the Experimental section. Data are represented as means ± SEM of 3 experiments performed in duplicate. Significant differences were calculated by Student's t-test for unpaired samples: * p < 0.05, ** p < 0.01 compared to untreated cells (basal).

Conclusions. We report the first adaptation of the indolo[2,3-*a*]quinolizidine privileged structure to solid-phase synthesis with the preparation of an 80-member indoloquinolizidine-

peptide library. In our library we explored peptides around the heterocyclic core to enhance the affinity of indoloquinolizidine-peptides at D₂R, a receptor that is crucial to re-establish activity on dopamine-depleted degenerated GABAergic neurons. Notably, we designed our library upon examination of the electrostatic potential at the extracellular regions of D₂R, which suggested that a positive charge at the C-terminal residue of indoloquinolizidine-peptides would enhance their affinity at D₂R. Binding assays identified a number of indoloquinolizidine-peptides with high affinity at both D₁R and D₂R. Compounds including a positively-charged amino acid at the C-terminus showed a significantly higher affinity at both receptors, and *trans* configuration at the indoloquinolizidine core significantly increased the selectivity towards D₂R. We identified **9a{1,3,3}** as a multiple D₁/D₂ ligand with some D₂R selectivity -micromolar affinity at D₁R and nanomolar affinity at D₂R- and studied the binding and functional properties at D₂R. Molecular dynamics simulations corroborated the proposed interactions between the indoloquinolizidine moiety and the orthosteric binding cavity as well as an ionic interaction between the C-terminal lysine and the anionic residues at the extracellular regions at D₂R. Furthermore, functional assays confirmed that **9a{1,3,3}** is an agonist of D₂R. These results validate the application of indoloquinolizidine-peptide combinatorial libraries as a platform to fine-tune the pharmacological profile of multiple ligands at D₁ and D₂ dopamine receptors.

Acknowledgements. We acknowledge the technical help obtained from Jasmina Jiménez (Molecular Neurobiology Laboratory, University of Barcelona) and from Serveis Científico-Tècnics of University of Barcelona for their support in the HRMS. This work was partially supported by grants from Spanish Government (SAF2008-03229-E, CTQ2008-00177, SAF2011-30508-C02-01, SAF2011-23813, and SAF2013-48271-C2-2-R), Fundació La Marató de TV3 (grant 060110), Generalitat de Catalunya (2009-SGR-1024 and 2009-SGR-12), CIBERBBN (CB06-01-0074), CIBERNED (CB06-05-0064) and the Barcelona Science

Park. M.V. acknowledges the support of the Medical Research Council (MRC) and the FP7 Marie Curie Integration Grant.

Electronic Supporting Information. Additional screening data, characterisation for the whole library of indoloquinolizidine-peptide, full characterisation data (HRMS, ^1H -NMR and ^{13}C -NMR) for **9a**{1,3,3} and **9b**{1,3,3}.

ACCEPTED MANUSCRIPT

Experimental section.

Materials and equipment. All Fmoc-amino acids were purchased from Neosystem (Strasbourg, France) and Fmoc-Rink-PS resin was supplied by Calbiochem-Novabiochem AG. DIC was obtained from Fluka (Buchs, Switzerland) and HOBt from Albatross Chem, Inc. (Montreal, Canada). Solvents for peptide synthesis and RP-HPLC equipment were obtained from Scharlau (Barcelona, Spain). Trifluoroacetic acid was supplied by KaliChemie (Bad Wimpfen, Germany). Other chemicals of the highest commercially available purity were purchased from Aldrich (Milwaukee, WI). All commercial reagents and solvents were used as received. Adenosine deaminase (EC 3.5.4.4) was purchased from Roche (Basel, Switzerland) and [³H]-R-PIA was supplied by Amersham Biosciences (Buckinghamshire, UK). Raclopride, polyethylenimine (PEI), MgCl₂, DPCPX, mouse anti-phospho-ERK1/2 antibody and rabbit anti-ERK1/2 antibody were purchased from Sigma (St Louis, MO). Rabbit anti-P-Ser⁴⁷³Akt antibody was purchased from SAB Signalway (Pearland, U.S.A.). ZM241385 and SCH 23390 were supplied by Tocris Biosciences (Avonmouth, UK). [³H]-SCH 23390, [³H]-YM 09151-2 and [³H]-ZM 241385 were supplied by Perkin Elmer (Wellesley, MA, USA). Ecoscint H scintillation cocktail was purchased from National Diagnostics (Atlanta, GA, USA). Bradford assay kit was purchased from Bio-Rad (Munich, Germany). All other supplements were purchased from Invitrogen (Paisley, UK). Analytical RP-HPLC-MS was performed using 2795 Waters (Milford, MA) Alliance with a Micromass ZQ Mass Spectrometer and a 996 PDA detector. Semi-preparative RP-HPLC was performed on a 2767 Waters chromatography system with a Micromass ZQ Mass Spectrometer. Multiple sample evaporation was carried out in a Discovery SpeedVac ThermoSavant (Waltham, MA). Radioligand binding experiments were performed using a Brandel (Gaithersburg, MD) cell harvester and a Packard 1600 TRI-CARB scintillation counter with an efficiency of 62%. Fitting data binding program GraFit was obtained from Erithacus

Software (Surrey, UK). For ERK1/2 phosphorylation determination, the Odyssey infrared scanner (LI-COR Biosciences, Lincoln, Nebraska, USA) was used. Band densities were quantified using the scanner software and exported to Excel (Microsoft, Redmond, WA, US).

Solid-phase general procedures. Peptide syntheses were performed manually in polypropylene syringes, each fitted with a polyethylene porous disk. Solvents and soluble reagents were removed by filtration. Washings between deprotection, coupling and subsequent deprotection steps were carried out with DMF (5×1 min) and DCM (5×1 min) using 10 mL of solvent/g of resin each time.

Coupling using DIC and HOBt or HOAt. Carboxylic acids (3 equiv) were coupled using DIC (3 equiv) as coupling reagent and HOBt (3 equiv) or HOAt (3 equiv) as additives in DCM-DMF (1:1) for 2 h at r.t. After each coupling, the resin was washed with DMF (5×1 min) and DCM (5×1 min). Reaction completion was checked by means of the Kaiser or chloranil tests.

Fmoc group removal. (i) DMF (5×1 min); (ii) piperidine-DMF (2:8) (1×1 min + 2×15 min); (iii) DMF (5×1 min).

Cleavage of the resins. The resins were treated with solutions of TFA-H₂O-DCM (95:2.5:2.5) or TFA-H₂O-DCM (30:5:65) and orbitally shaken for 1 h at r.t. Filtrates were collected, washed with TFA (2×1 min) and DCM (3×1 min) and evaporated under vacuum.

Purification of the library. A) Solid-phase extraction purification. Crudes were dissolved in a mixture of DCM-MeOH (1:1, v/v) and loaded onto a SCX-2 column previously conditioned with a mixture of DCM-MeOH (1:1, v/v). Impurities were eluted with DCM-MeOH and the products were liberated from the column with a solution of NH₃ in MeOH.

B) RP-HPLC-MS purification. A small portion of the library was purified by semi-preparative RP-HPLC-MS using a reversed-phase Symmetry C₁₈ (30×100 mm², 5 μ m)

column. Elution system: A: H₂O/HCOOH, 99.9:0.1; B: CH₃CN/HCOOH, 99.9:0.1. Flow rate: 25 mL·min⁻¹. Purification gradient: 0-50% or 0-55% B over 30 min.

Synthesis of the indoloquinolizidine-peptide library. The 80-member library synthesis was carried out in a MiniBlock reactor. For each of the 20 chemsets, 400 mg of Fmoc-Rink-MBHA resin (0.7 mmol·g⁻¹) were swollen with DCM (1 × 1 min, 2 × 10 min) and DMF (5 × 1 min, 1 × 15 min) before use. After washing, the Fmoc group was removed and the 3 amino acids were coupled as above mentioned. At this point, resins were split into two equal aliquots and Fmoc-Ahx-OH was coupled to half the library using DIC and HOBt. Chemset resins **4** and **5** were thoroughly washed and divided again in two parts, obtaining at that point 80 syringes with 100 mg of resin each. A solution of **1** (1.6 g, 7 mmol, 2.5 equiv), PyBOP (3.6 g, 7 mmol, 2.5 equiv) and HOAt (1 g, 7 mmol, 2.5 equiv) in 40 mL of DMF was prepared. Similarly, a solution of **2** (1.2 g, 7 mmol, 2.5 equiv), PyBOP (2.8 g, 5.6 mmol, 2 equiv) and HOAt (0.8 g, 5.6 mmol, 2 equiv) in 40 mL of DMF was prepared. For each of the acids, 1 mL of the aforementioned solution was added to each of the 40 chemset resins together with DIPEA (63 μL, 0.35 mmol, 5 equiv), and the 80 resins were stirred for 2 h at r.t. Cleavages were performed as described above. Multiple evaporation in the ThermoSavant Discovery SpeedVac rendered the crude mixtures that were further purified as above mentioned.

Scale-up of 9{1,3,3}. Fmoc-Rink-MBHA resin (0.2 g, 0.112 mmol, 0.56 mmol/g) was swollen in DCM (1 × 1 min, 2 × 10 min) before used and treated with piperidine to remove the Fmoc group as previously described. Amino acids (3 equiv) were coupled using DIC (3 equiv) and HOBt (3 equiv) in DCM:DMF (1:1) for 2 h at r.t. or using PyBOP (3 equiv), HOBt (3 equiv) and DIPEA (6 equiv) for 1-2 h. After each coupling the resin was washed with DMF (5 × 1 min) and DCM (5 × 1 min). Reaction completion was monitored by Kaiser or chloranil tests. For the coupling of the indolo[2,3-*a*]quinolizidine structure, we used the

racemic mixture **2** (Figure 1a). After coupling, the resulting mixture was cleaved as indicated above and purified by semi-preparative RP-HPLC-MS. The two *trans* diastereoisomers (**9a**{1,3,3} and **9b**{1,3,3}) were isolated and used separately in biological assays. Full characterisation data for compounds **9a**{1,3,3} and **9b**{1,3,3} is included in the Electronic Supporting Information (ESI).

Radioligand binding experiments: general procedure. Membrane suspensions from sheep striatum were obtained following methods described previously.^{25,26} Tissue was disrupted with a Polytron homogenizer (PTA 20 TS rotor, setting 3; Kinematica, Basel, Switzerland) for three 5 s-periods in 10 volumes of 50 mM Tris-HCl buffer, pH 7.4 containing a proteinase inhibitor cocktail (Sigma, St. Louis, MO, USA). Cell debris were eliminated and membranes were obtained by centrifugation at 105,000 g (40 min, 4 °C), and the pellet was resuspended and recentrifuged under the same conditions. The pellet was stored at -80 °C and was washed once more as described above and resuspended in 50 mM Tris-HCl buffer for immediate use. Protein was quantified by the bicinchoninic acid method (Pierce Chemical Co., Rockford, IL, USA) using bovine serum albumin dilutions as standard.

Radioligand binding assays of membrane suspensions (0.2-0.3 mg protein•mL⁻¹) were carried out at 25°C in 50 mM Tris-HCl buffer (pH 7.4) containing 10 mM MgCl₂ and 0.2-2 U/mL adenosine deaminase (ADA) with the indicated concentrations (see conditions used for each receptor below). After radioligand incubation, free and membrane-bound ligand were separated by rapid filtration of 500 µL aliquots in a cell harvester through Whatman GF/C filters embedded in polyethylenimine (0.3%) that were subsequently washed for 5 s with 5 mL of ice-cold Tris-HCl buffer.²⁵ Nonspecific binding was determined with non-labeled ligands at the concentration indicated below. In all cases, the filters were incubated with 10 mL Ecoscint H scintillation cocktail overnight at r.t. Radioactivity counts in the vials were determined using a scintillation counter.

Library screening. Initial binding experiments of the whole library were performed at a concentration of 50 μM for all compounds.

D₁R. Membranes were incubated with 2 nM [³H]-SCH 23390 (85 Ci mmol⁻¹) in 50 mM Tris-HCl buffer (pH 7.4) containing 10 mM MgCl₂ for 1.5 h in the presence or in the absence of the tested compounds. Nonspecific binding was measured in the presence of 50 μM SCH 23390.

D₂R. Membranes were incubated with 2 nM [³H]-YM 09151-2 (85.5 Ci mmol⁻¹) in 50 mM Tris-HCl buffer (pH 7.4) containing 10 mM MgCl₂ for 2 h in the presence or in the absence of the tested compounds. Nonspecific binding was measured in the presence of 50 μM raclopride.

A₁R. Membranes were incubated with 1 nM [³H]-R-PIA (30.5 Ci mmol⁻¹) in 50 mM Tris-HCl buffer (pH 7.4) containing 10 mM MgCl₂ and 0.2 U mL⁻¹ ADA for 2 h in the presence or in the absence of the tested compounds. Nonspecific binding was measured in the presence of 50 μM DPCPX.

A_{2A}R. Membranes were incubated with 1 nM [³H]-ZM 241385 (27.4 Ci mmol⁻¹) in 50 mM Tris-HCl buffer (pH 7.4) containing 10 mM MgCl₂ and 2 U mL⁻¹ ADA for 1.5 h in the presence or in the absence of the tested compounds. Nonspecific binding was measured in the presence of 50 μM ZM-241385.

K_D determination. Competition experiments were performed by incubating membranes under the same conditions as described above, in the absence or presence of increasing concentrations of the 10 selected indoloquinolizidine-peptide hybrids ((**9**{2,2,2}, **9**{2,4,2}, **7**{2,1,3}, **9**{1,2,3}, **7**{2,2,3}, **9**{1,3,3}, **7**{2,3,3}, **9**{2,4,3}, **6**{2,4,2}, **8**{2,1,3})) for D₁R and D₂R. Nonspecific binding was determined as previously outlined. Radioligand displacement curves were analyzed by nonlinear regression using the commercial program GraFit (Erithacus Software, Surrey, UK) by fitting the total binding data to the displacement models with one

or two affinity sites.^{27,28} Goodness of fit was tested following the reduced χ^2 value given by the nonlinear regression program in GraFit. A modified F test was used to analyze whether the fit to the two-site model significantly improved on the fit to the one-site model, and $p < 0.05$ was taken as a criterion of significance; when no significant improvement over the one-site model was detected, the p values were > 0.30 .

Biological characterisation of 9a{1,3,3} and 9b{1,3,3}. For competition assays of compounds **9a{1,3,3}** and **9b{1,3,3}** membrane suspensions (0.2–0.5 mg protein/mL) were prepared as previously described and incubated 2 h at 25°C in 50 mM Tris–HCl buffer, pH 7.4, containing 10 mM MgCl₂ with the indicated free concentration of the D₁ receptor antagonist [³H]-SCH 23390 or with the indicated free concentration of the D₂ receptor antagonist [³H]-YM 09151-2 and increasing concentrations of **9a{1,3,3}** or **9b{1,3,3}** (triplicates of 9 different concentrations from 1 nM to 50 μM). Nonspecific binding was determined in the presence of 50 μM SCH 23390 or 50 μM raclopride, and confirmed that the value was the same as calculated by extrapolation of the competition curves.

For dissociation kinetic assays, sheep brain striatum membranes (0.2 mg of protein/mL) were incubated for 1 h at 25 °C with or without 3 μM of **9a{1,3,3}** in Tris-HCl buffer (50 mM, pH 7.4) containing 10 mM MgCl₂ before adding 1 nM [³H]-YM 09151-2. After 2 h the dissociation was initiated by the addition of 10 μM YM 09151-2. At the indicated time interval total binding was measured by rapid filtration and determination of radioactivity counts as indicated above. Nonspecific binding was measured after 90 min incubation in the presence of 10 μM YM 09151-2.

Cell culture and transient transfection. CHO cells, grown as previously described,^{26,29} were transiently transfected with D₂R cDNA by Lipofectamine (Invitrogen) following the instructions of the supplier. Cells were used 48 h after transfection.

ERK1/2 phosphorylation assays. Transfected CHO cells were cultured in serum-free

medium for 16 h before the addition of the indicated concentration of ligands for the indicated time. Cells and slices were lysed in ice-cold lysis buffer and ERK1/2 phosphorylation was determined as indicated elsewhere.²⁹

Molecular modeling. Modeller v9.10³⁰ was used to build a homology model of human D₂R (Uniprot code P14416) using the crystal structure of the dopamine D₃R (PDB code 3PBL)³¹ as template. **9a{1,3,3}** was docked by interactive computer graphics, using PyMol,³² into the receptor model with its protonated NH group of the ring interacting with D114^{3,32}. This structure was placed in a rectangular box containing a lipid bilayer (182 molecules of POPC) with explicit solvent (14335 water molecules) and a 0.15 M concentration of Na⁺ and Cl⁻ ions. This initial complex was energy minimized and subsequently subjected to a 10 ns MD equilibration, with positional restraints on protein coordinates, to remove possible voids present in protein/lipids or proteins/water interfaces. These restraints were released, and 200 ns MD trajectories were produced at constant pressure and temperature, using the particle mesh Ewald method to evaluate electrostatic interactions. Computer simulations were performed with the GROMACS 4.5.3 simulation package,³³ using the AMBER99SB force field³⁴ as implemented in GROMACS, Berger parameters for POPC lipids,³⁵ and the general Amber force field (GAFF)³⁶ and HF/6-31G*-derived RESP atomic charges for the ligand. This procedure has been previously validated.³⁷ The molecular electrostatic potential on the extracellular surface was calculated and displayed with the program VASCo 1.02.³⁸

References

- (1) Cironi, P.; Alvarez, M.; Albericio, F. *Mini Rev. Med. Chem.* **2006**, *6*, 11.
- (2) Sanchez-Martin, R. M.; Mittoo, S.; Bradley, M. *Curr. Top. Med. Chem.* **2004**, *4*, 653.
- (3) Lee, T.; Gong, Y. D. *Molecules* **2012**, *17*, 5467.
- (4) Nandy, J. P.; Prakesch, M.; Khadem, S.; Reddy, P. T.; Sharma, U.; Arya, P. *Chem. Rev.* **2009**, *109*, 1999.
- (5) Vendrell, M.; Zhai, D.; Er, J. C.; Chang, Y. T. *Chem. Rev.* **2012**, *112*, 4391.
- (6) Vendrell, M.; Krishna, G. G.; Ghosh, K. K.; Zhai, D.; Lee, J. S.; Zhu, Q.; Yau, Y. H.; Shochat, S. G.; Kim, H.; Chung, J.; Chang, Y. T. *Chem. Commun.* **2011**, *47*, 8424.
- (7) Guo, T.; Hobbs, D. W. *Assay Drug Dev. Technol.* **2003**, *1*, 579.
- (8) de Sa Alves, F. R.; Barreiro, E. J.; Fraga, C. A. *Mini Rev. Med. Chem.* **2009**, *9*, 782.
- (9) Mercuri, N. B.; Bernardi, G. *Trends Pharmacol. Sci.* **2005**, *26*, 341.
- (10) Schapira, A. H.; Bezard, E.; Brotchie, J.; Calon, F.; Collingridge, G. L.; Ferger, B.; Hengerer, B.; Hirsch, E.; Jenner, P.; Le Novere, N.; Obeso, J. A.; Schwarzschild, M. A.; Spampinato, U.; Davidai, G. *Nat. Rev. Drug Discovery* **2006**, *5*, 845.
- (11) Obeso, J. A.; Rodriguez-Oroz, M. C.; Benitez-Temino, B.; Blesa, F. J.; Guridi, J.; Marin, C.; Rodriguez, M. *Mov. Disord.* **2008**, *23* S3, S548.
- (12) Vendrell, M.; Angulo, E.; Casadó, V.; Lluís, C.; Franco, R.; Albericio, F.; Royo, M. *J. Med. Chem.* **2007**, *50*, 3062.
- (13) Vendrell, M.; Molero, A.; Gonzalez, S.; Perez-Capote, K.; Lluís, C.; McCormick, P. J.; Franco, R.; Cortes, A.; Casadó, V.; Albericio, F.; Royo, M. *J. Med. Chem.* **2011**, *54*, 1080.
- (14) Soriano, A.; Vendrell, M.; Gonzalez, S.; Mallol, J.; Albericio, F.; Royo, M.; Lluís, C.; Canela, E. I.; Franco, R.; Cortes, A.; Casadó, V. *J. Pharmacol. Exp. Ther.* **2010**, *332*, 876.
- (15) Vendrell, M.; Soriano, A.; Casadó, V.; Diaz, J. L.; Lavilla, R.; Canela, E. I.; Lluís, C.; Franco, R.; Albericio, F.; Royo, M. *ChemMedChem* **2009**, *4*, 1514.
- (16) Hoefgen, B.; Decker, M.; Mohr, P.; Schramm, A. M.; Rostom, S. A.; El-Subbagh, H.; Schweikert, P. M.; Rudolf, D. R.; Kassack, M. U.; Lehmann, J. *J. Med. Chem.* **2006**, *49*, 760.
- (17) Wenkert, E.; Moeller, P. D. R.; Shi, Y. J. *J. Org. Chem.* **1988**, *53*, 2383 and references cited therein.
- (18) Sealfon, S. C.; Chi, L.; Ebersole, B. J.; Rodic, V.; Zhang, D.; Ballesteros, J. A.; Weinstein, H. *J. Biol. Chem.* **1995**, *270*, 16683.
- (19) Woodward, R. B. B., F. E.; Bickel, H.; Frey, A. J.; Kierstead, R. W. *J. Am. Chem. Soc.* **1956**, *78*, 2023.
- (20) Woodward, R. B. B., F. E.; Bickel, H.; Frey, A. J.; Kierstead, R. W. *Tetrahedron* **1958**, *2*, 1.
- (21) Yraola, F. V., R.; Vendrell, M.; Colombo, A.; Fernández, J. C.; de la Figuera, N.; Fernández-Fórner, D.; Royo, M.; Forns, P.; Albericio, F. *QSAR & Comb. Sci.* **2004**, *23*, 145.
- (22) Berthet, A.; Bezard, E.; Porrás, G.; Fasano, S.; Barroso-Chinea, P.; Dehay, B.; Martínez, A.; Thiolat, M. L.; Nosten-Bertrand, M.; Giros, B.; Baufreton, J.; Li, Q.; Bloch, B.; Martin-Negrier, M. L. *J. Neurosci.* **2012**, *32*, 681.
- (23) Fieblinger, T.; Sebastianutto, I.; Alcacer, C.; Bimpisidis, Z.; Maslava, N.; Sandberg, S.; Engblom, D.; Cenci, M. A. *J. Neurosci.* **2014**, *34*, 4728.
- (24) Gonzalez, A.; Perez-Acle, T.; Pardo, L.; Deupi, X. *PloS One* **2011**, *6*, e23815.
- (25) Sarrió, S.; Casadó, V.; Escriche, M.; Ciruela, F.; Mallol, J.; Canela, E. I.; Lluís, C.; Franco, R. *Mol. Cell Biol.* **2000**, *20*, 5164.
- (26) Ferrada, C.; Moreno, E.; Casadó, V.; Bongers, G.; Cortes, A.; Mallol, J.; Canela, E. I.; Leurs, R.; Ferre, S.; Lluís, C.; Franco, R. *Br. J. Pharmacol.* **2009**, *157*, 64.
- (27) Cheng, Y. C.; Prusoff, W. H. *Biochem. Pharmacol.* **1973**, *22*, 3099.

- (28) Casadó, V.; Casillas, T.; Mallol, J.; Canela, E. I.; Lluís, C.; Franco, R. *J. Neurochem.* **1992**, *59*, 425.
- (29) Navarro, G.; Aymerich, M. S.; Marcellino, D.; Cortes, A.; Casadó, V.; Mallol, J.; Canela, E. I.; Agnati, L.; Woods, A. S.; Fuxe, K.; Lluís, C.; Lanciego, J. L.; Ferre, S.; Franco, R. *J. Biol. Chem.* **2009**, *284*, 28058.
- (30) Marti-Renom, M. A.; Stuart, A. C.; Fiser, A.; Sanchez, R.; Melo, F.; Sali, A. *Annu. Rev. Biophys. Biomol. Struct.* **2000**, *29*, 291.
- (31) Chien, E. Y.; Liu, W.; Zhao, Q.; Katritch, V.; Han, G. W.; Hanson, M. A.; Shi, L.; Newman, A. H.; Javitch, J. A.; Cherezov, V.; Stevens, R. C. *Science* **2010**, *330*, 1091.
- (32) The PyMOL Molecular Graphics Version 1.5.0.4 Schrödinger, L.
- (33) Hess, B.; Kutzner, C.; van der Spoel, D.; Lindahl, E. *J. Chem. Theory Comput.* **2008**, *4*, 435.
- (34) Hornak, V.; Abel, R.; Okur, A.; Strockbine, B.; Roitberg, A.; Simmerling, C. *Proteins* **2006**, *65*, 712.
- (35) Berger, O.; Edholm, O.; Jahnig, F. *Biophys. J.* **1997**, *72*, 2002.
- (36) Wang, J.; Wolf, R. M.; Caldwell, J. W.; Kollman, P. A.; Case, D. A. *J. Comput. Chem.* **2004**, *25*, 1157.
- (37) Cordini, A.; Caltabiano, G.; Pardo, L. *J. Chem. Theory Comput.* **2012**, *8*, 948.
- (38) Steinkellner, G.; Rader, R.; Thallinger, G.; Kratky, C.; Gruber, K. *BMC Bioinformatics* **2009**, *10*, 32.

Table 1. Optimisation of the coupling of indolo[2,3-*a*]quinolizidine carboxylic acids **1** and **2** to solid support.

Acid	Supported amine	Coupling conditions	Reaction time (h)	Purity*
1	Rink-MBHA-PS	DIC, HOAt	16	39
1	Rink-MBHA-PS	PyBOP, HOAt, DIPEA	2	90
2	Rink-MBHA-PS	DIC, HOAt	16	35
2	Rink-MBHA-PS	PyBOP, HOAt, DIPEA	2	92
1	Glu-Trp-Pro-PS'	PyBOP, HOAt, DIPEA	2	95
2	Glu-Trp-Pro-PS'	PyBOP, HOAt, DIPEA	2	92
1	Pro-Tyr-Lys-PS'	PyBOP, HOAt, DIPEA	2	93
2	Pro-Tyr-Lys-PS'	PyBOP, HOAt, DIPEA	2	95

* Determined by HPLC monitoring UV-absorbance at 220 nm; PS: polystyrene; PS':Rink-MBHA-PS.

Table 2. K_D values (μM) of selected indoloquinolizidine-peptides at D_1R and D_2R .[‡]

Code	Description	D_1R	D_2R	
			K_{D1}	K_{D2}
6{2,4,2}	<i>cis</i> {Nle-Phe(4F)-Amp}	27 \pm 2	5.0 \pm 0.5	--
8{2,1,3}	<i>cis</i> -spacer{Nle-Tyr-Lys}	38 \pm 3	6.3 \pm 0.7	--
9{1,2,3}	<i>trans</i> -spacer{Pro-Trp-Lys}	2.9 \pm 0.7	0.24 \pm 0.09	7 \pm 2
9{1,3,3}	<i>trans</i> -spacer{Pro-Phe(3,4-F2)-Lys}	15 \pm 1	0.28 \pm 0.08	9 \pm 3
7{2,1,3}	<i>trans</i> {Nle-Tyr-Lys}	1.2 \pm 0.1	4.7 \pm 0.7	--
9{2,2,2}	<i>trans</i> -spacer{Nle-Trp-Amp}	3.4 \pm 0.3	0.6 \pm 0.2	20 \pm 10
7{2,2,3}	<i>trans</i> {Nle-Trp-Lys}	1.9 \pm 0.4	0.9 \pm 0.2	16 \pm 4
7{2,3,3}	<i>trans</i> {Nle-Phe(3,4-F2)-Lys}	1.3 \pm 0.2	0.19 \pm 0.06	8 \pm 3
9{2,4,2}	<i>trans</i> -spacer{Nle-Phe(4F)-Amp}	4.0 \pm 1.0	0.5 \pm 0.2	13 \pm 4
9{2,4,3}	<i>trans</i> -spacer{Nle-Phe(4F)-Lys}	3.3 \pm 0.7	2.0 \pm 1.0	--

[‡] Data are represented as means \pm SD of three different experiments performed in triplicate.

Table 3. K_D (μM) values of **9a**{1,3,3} and **9b**{1,3,3} at D_1R and D_2R .[†]

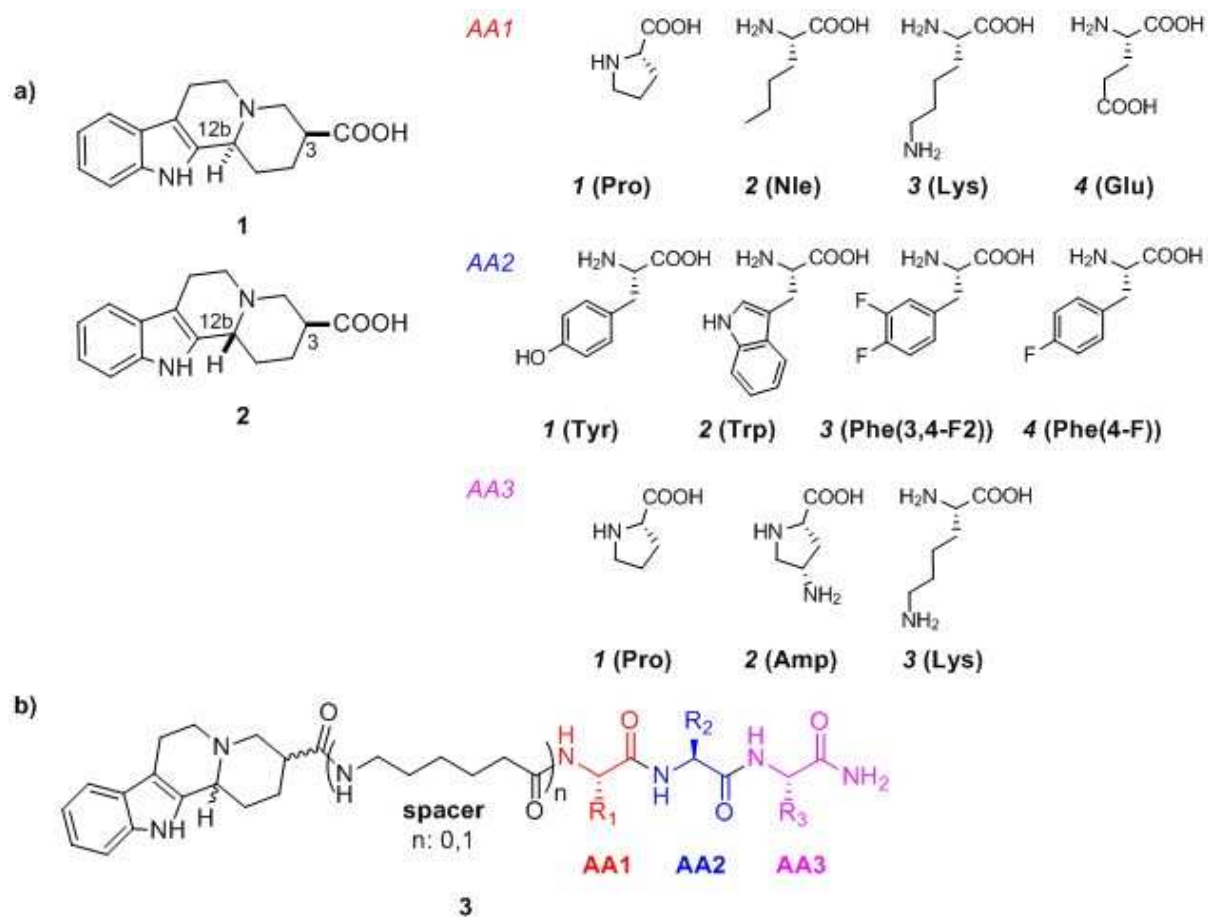
		B_{E1} (pmol/mg prot)	K_{D1} (μM)	B_{E2} (pmol/mg prot)	K_{D2} (μM)
D₁R	9a {1,3,3}	0.13±0.02	1.5±0.9	0.35±0.06	24±6
	9b {1,3,3}	0.14±0.05	1.6±0.8	0.24±0.05	30±7
D₂R	9a {1,3,3}	0.04±0.02	0.2±0.1	0.12±0.02	4±1
	9b {1,3,3}	0.06±0.02	0.4±0.2	0.12±0.02	14±5*

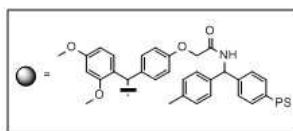
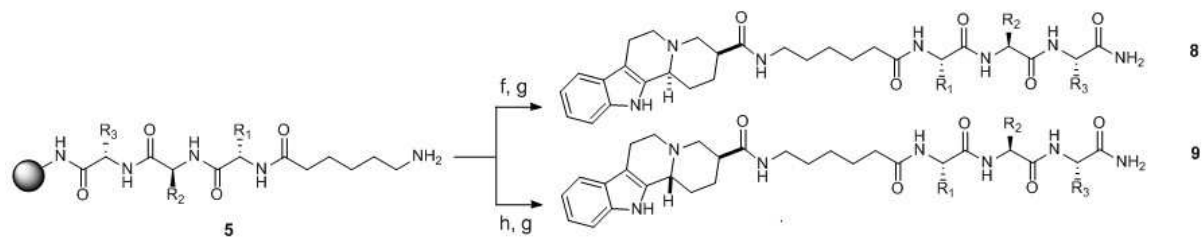
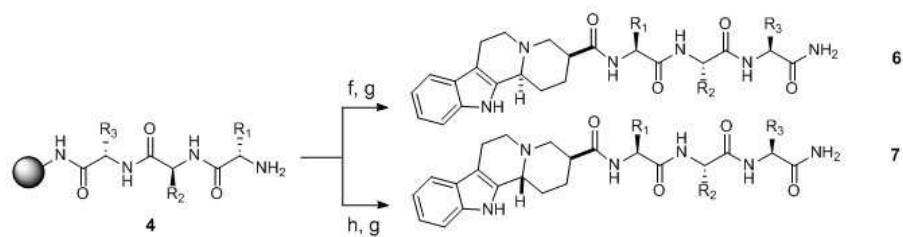
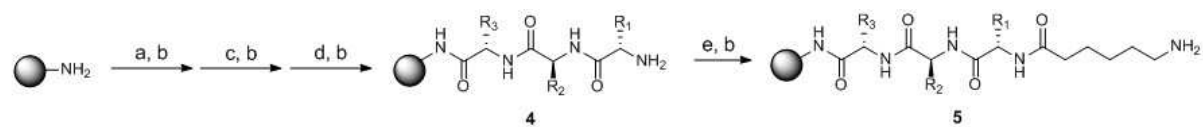
[†] Data are represented as means \pm SD of three different experiments performed in triplicate.

* Statistical significance ($p < 0.05$) was calculated by a Student's t-test compared to the K_{D2} value of **9a**{1,3,3}.

Table 4. Dissociation assay of [³H]-YM 09151-2 at D₂R in the presence of **9a**{1,3,3}.

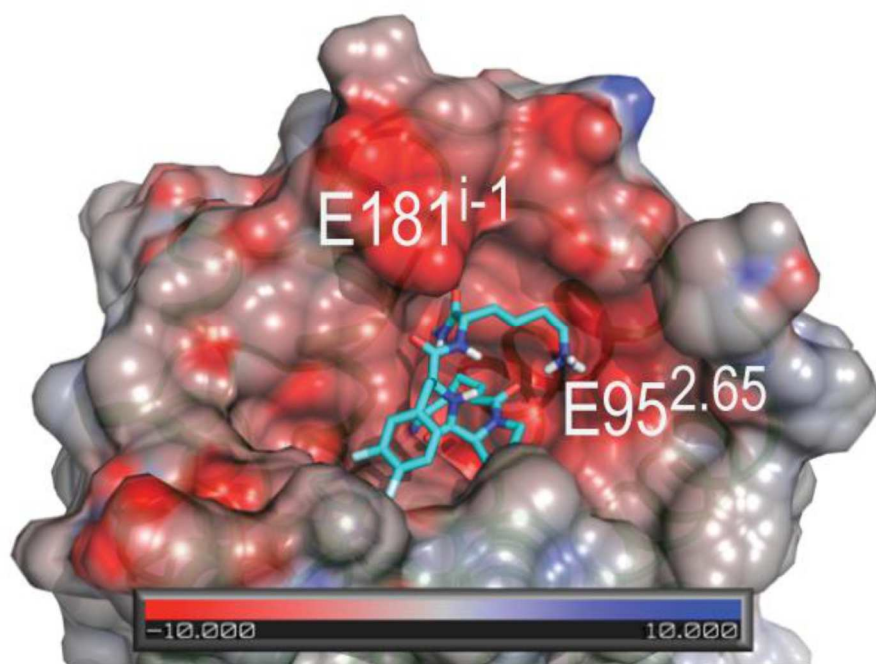
	B_E (pmol/mg prot)	K_{off} (min⁻¹)
[³ H]-YM 09151-2	0.21±0.01	0.018±0.002
[³ H]-YM 09151-2+ 9a {1,3,3}	0.13±0.02	0.018±0.004





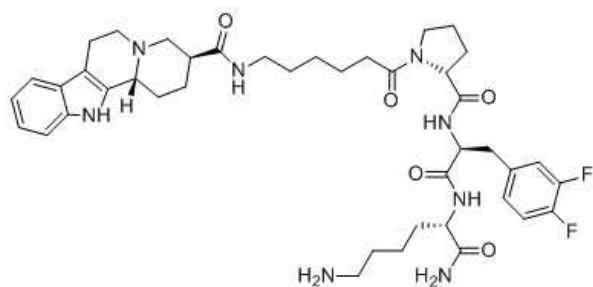
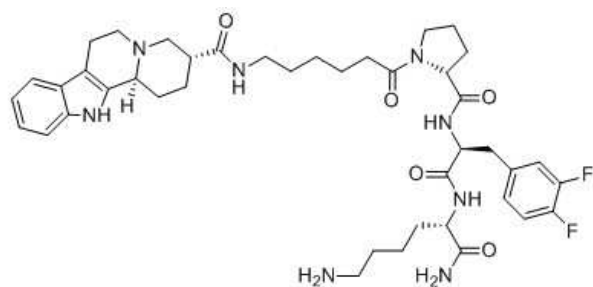
CODE FOR LIBRARY COMPOUNDS: 6-9 {AA1, AA2, AA3}

ACCEPTED MANUSCRIPT

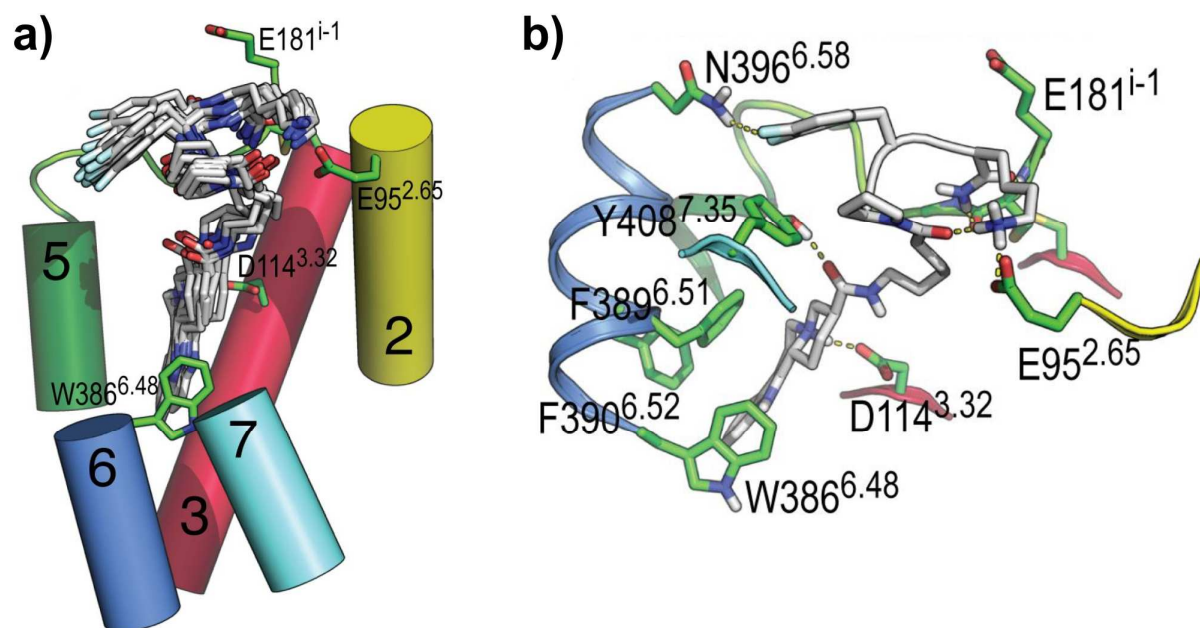


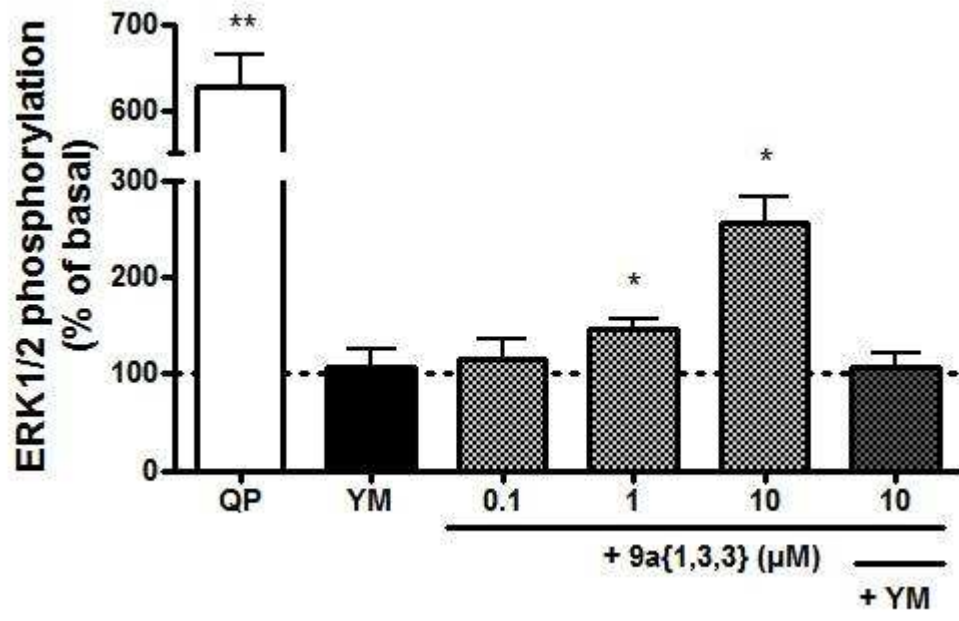
ACCEPTED MANUSCRIPT

SCRIPT

**9a{1,3,3}****9b{1,3,3}**

ACCEPTED MANUSCRIPT





Highlights

A Solid-Phase Combinatorial Approach for Indoloquinolizidine-Peptides with High Affinity at D₁ and D₂ Dopamine Receptors

- Indolo[2,3-*a*]quinolizidines were used for the first time in solid-phase synthesis.
- A positively charged *C*-terminus in indoloquinolizidine-peptides enhances their affinity at D₂R.
- *Trans* configuration of the indoloquinolizidine increases selectivity towards D₂R.
- **9a{1,3,3}** is a D₁/D₂ ligand with submicromolar affinity at D₁R, and nanomolar affinity and agonist activity at D₂R.

Electronic Supporting Information**A Solid-Phase Combinatorial Approach for Indoloquinolizidine-Peptides with High Affinity at D₁ and D₂ Dopamine Receptors**

Anabel Molero, Marc Vendrell, Jordi Bonaventura, Julian Zachmann, Laura López, Leonardo Pardo, Carme Lluís, Antoni Cortés, Fernando Albericio, Vicent Casadó and Miriam Royo

Table of contents:

1. Stability assays for indolo[2,3-*a*]quinolizidine carboxylic acids **1** and **2**.
2. Characterisation data for the whole library.
3. High-throughput binding screening of the whole library at D₁R and D₂R.
4. Screening of selected indoloquinolizidine-peptides at A₁ and A_{2A} adenosine receptors.
5. Binding curves for **9a**{1,3,3} and **9b**{1,3,3} at D₁R and D₂R.
6. Full characterisation data for **9a**{1,3,3} and **9b**{1,3,3}.

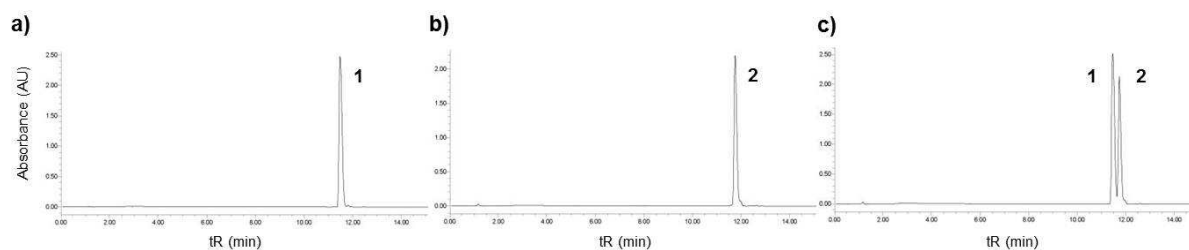
1. Stability assays for indolo[2,3-*a*]quinolizidine carboxylic acids **1 and **2**.**

Figure S1. HPLC characterisation of acids **1** and **2** after treatment with TFA:H₂O:DCM (95:2.5:2.5). a) HPLC of acid **1**; b) HPLC of acid **2**; c) co-elution of acids **1** and **2**. HPLC conditions: Symmetry C₁₈ column (4.6 × 75 mm, 5μm), 0-60% B in 15 min, (A:H₂O-TFA (99.9:0.1), B: ACN-TFA (99.9:0.1)), flow: 1 mL min⁻¹, detection at 220 nm.

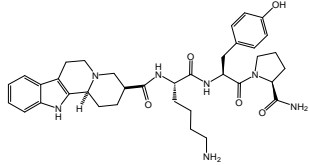
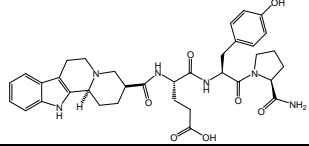
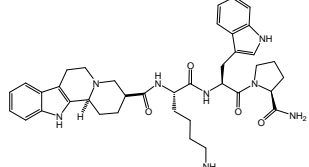
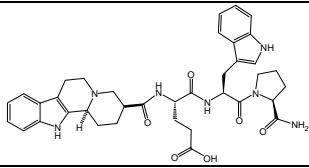
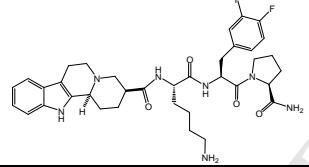
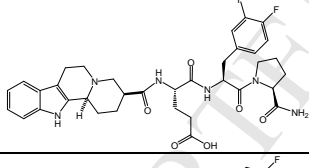
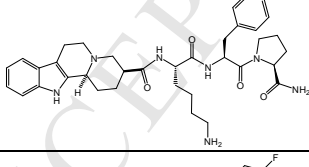
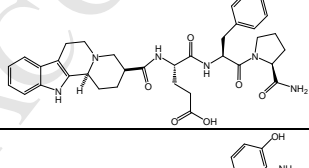
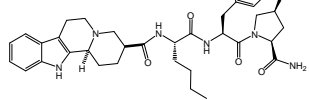
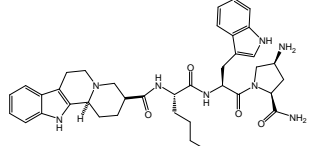
2. Characterisation data for the whole library.

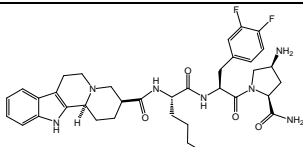
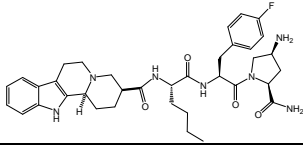
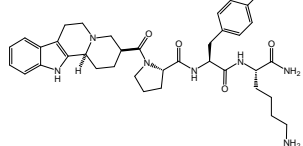
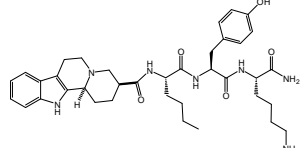
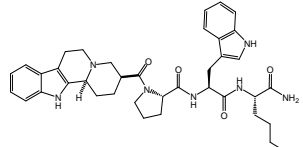
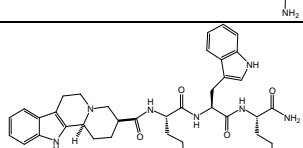
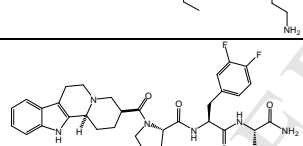
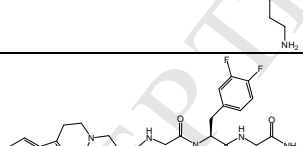
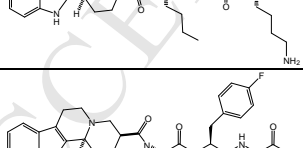
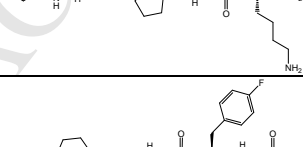
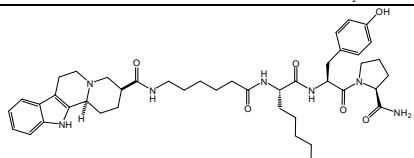
Table S1. HPLC purities of the whole library of indoloquinolizidine-peptides.

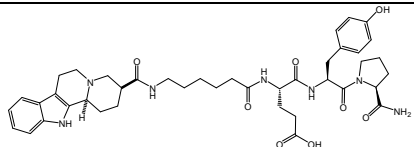
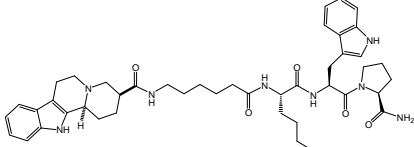
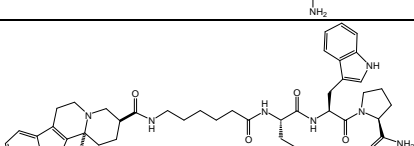
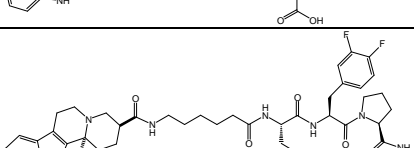
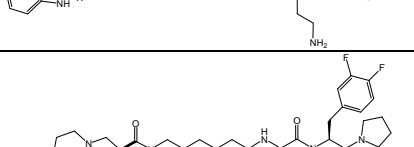
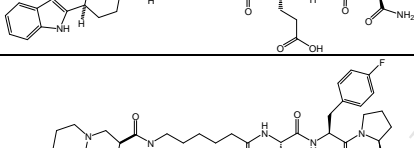

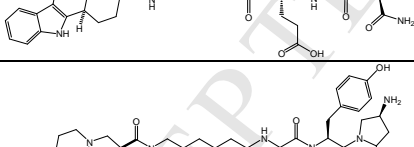
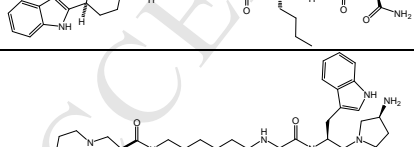
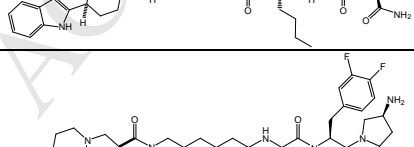
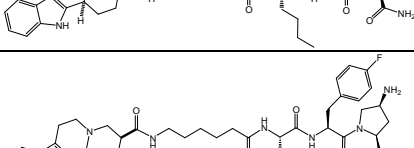
compound	mg	purity (sist ₁ %-sist ₂ %)*	compound	mg	purity (sist ₁ %-sist ₂ %)*
6{1,1,3}	3.7	94%-96%	7{1,1,3}	5.7	94%-92%
6{1,2,3}	10.8	97%-95%	7{1,2,3}	6.9	98%-97%
6{1,3,3}	4.1	95%-95%	7{1,3,3}	4.3	98%-96%
6{1,4,3}	4.0	92%-90%	7{1,4,3}	4.8	98%-92%
6{2,1,2}	0.8	97%-93%	7{2,1,2}	35.4	91%-80%
6{2,1,3}	7.7	94%-96%	7{2,1,3}	6.3	93%-95%
6{2,2,2}	2.7	99%-93%	7{2,2,2}	6.0	94%-96%
6{2,2,3}	5.3	97%-95%	7{2,2,3}	8.6	99%-98%
6{2,3,2}	0.6	93%-95%	7{2,3,2}	0.6	97%-95%
6{2,3,3}	7.2	95%-89%	7{2,3,3}	5.5	94%-91%
6{2,4,2}	0.5	88%-90%	7{2,4,2}	0.8	90%-90%
6{2,4,3}	6.9	90%-88%	7{2,4,3}	9.8	91%-85%
6{3,1,1}	15.7	91%-93%	7{3,1,1}	78.0	99%-94%
6{3,2,1}	26.2	97%-95%	7{3,2,1}	30.7	94%-91%
6{3,3,1}	17.4	95%-95%	7{3,3,1}	17.6	99%-98%
6{3,4,1}	22.1	87%-83%	7{3,4,1}	7.4	98%-96%
6{4,1,1}	54.5	92%-89%	7{4,1,1}	6.6	90%-90%
6{4,2,1}	44.9	91%-88%	7{4,2,1}	10.3	92%-91%
6{4,3,1}	54.9	96%-92%	7{4,3,1}	64.8	96%-93%
6{4,4,1}	53.9	90%-92%	7{4,4,1}	17.6	92%-89%
8{1,1,3}	2.7	89%-90%	9{1,1,3}	1.2	99%-98%
8{1,2,3}	4.7	93%-94%	9{1,2,3}	7.3	99%-97%
8{1,3,3}	2.5	91%-90%	9{1,3,3}	5.3	93%-91%
8{1,4,3}	22.0	85%-88%	9{1,4,3}	3.5	93%-98%
8{2,1,2}	0.8	82%-85%	9{2,1,2}	1.0	84%-89%
8{2,1,3}	4.6	85%-87%	9{2,1,3}	5.5	91%-94%
8{2,2,2}	0.4	92%-98%	9{2,2,2}	1.2	96%-93%
8{2,2,3}	3.4	83%-86%	9{2,2,3}	2.4	85%-92%
8{2,3,2}	0.5	80%-88%	9{2,3,2}	5.9	85%-86%
8{2,3,3}	0.7	99%-98%	9{2,3,3}	2.1	99%-99%
8{2,4,2}	1.0	92%-90%	9{2,4,2}	0.6	81%-83%
8{2,4,3}	1.5	96%-98%	9{2,4,3}	4.0	83%-80%
8{3,1,1}	13.2	80%-88%	9{3,1,1}	15.1	80%-89%
8{3,2,1}	8.0	85%-95%	9{3,2,1}	16.8	93%-94%
8{3,3,1}	6.6	91%-92%	9{3,3,1}	7.3	99%-99%
8{3,4,1}	5.0	91%-90%	9{3,4,1}	9.7	95%-86%
8{4,1,1}	4.3	98%-99%	9{4,1,1}	0.7	99%-99%
8{4,2,1}	68.4	79%-94%	9{4,2,1}	42.9	89%-87%
8{4,3,1}	1.9	99%-99%	9{4,3,1}	2.6	99%-83%
8{4,4,1}	1.7	99%-99%	9{4,4,1}	8.1	99%-99%

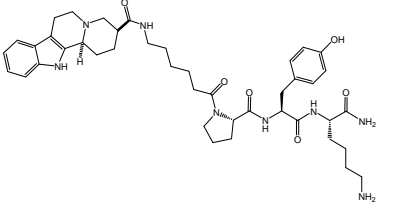
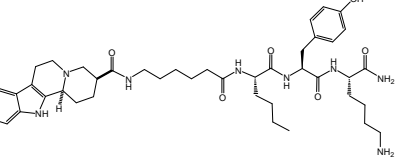
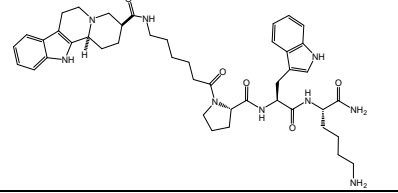
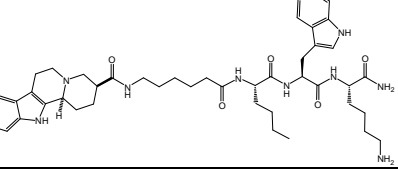
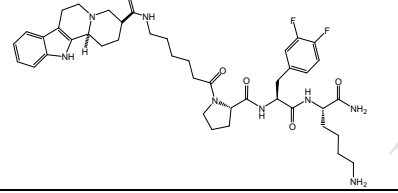
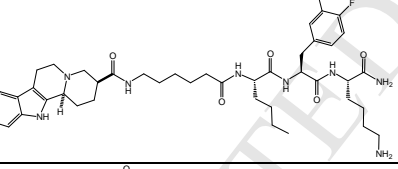
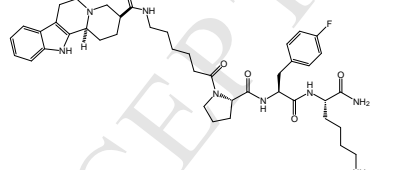
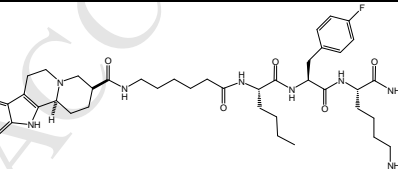
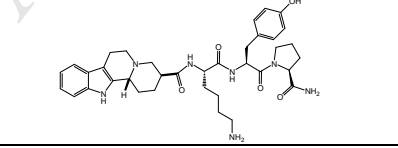
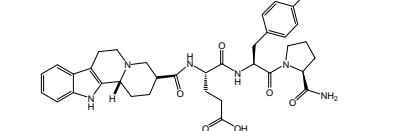
*Sist₁: HPLC conditions: Symmetry C₁₈ column (4.6 × 75 mm, 5μm), 0-60% B in 10 min, (A: H₂O-TFA (99.9:0.1), B: ACN-TFA (99.9:0.1)), flow: 1 mL min⁻¹, detection at 220 nm. *Sist₂: HPLC conditions: Symmetry C₁₈ column (4.6 × 75 mm, 5μm), 0-60% B in 10 min, (A: H₂O-HCOOH (99.9:0.1), B: ACN-HCOOH (99.93:0.07)), flow: 1 mL min⁻¹, detection at 220 nm.

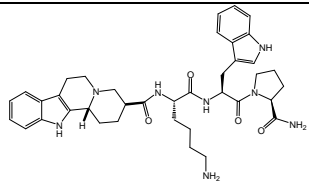
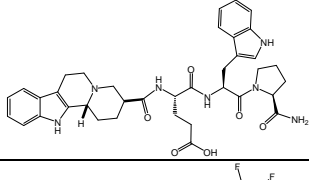
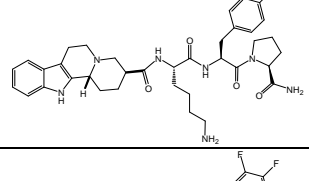
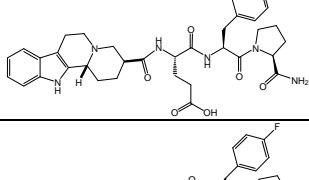
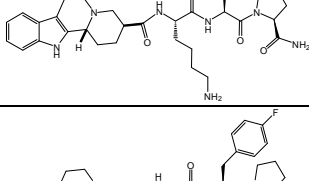
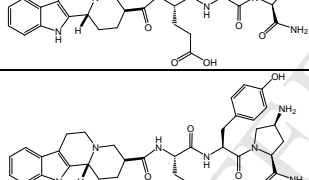
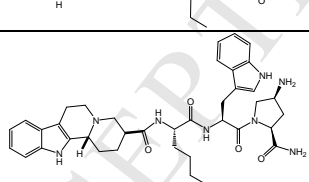
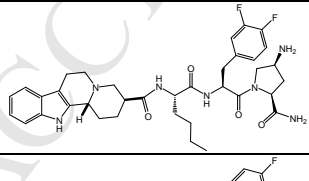
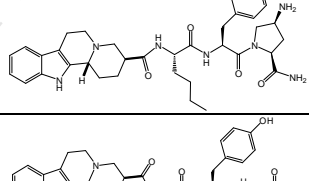
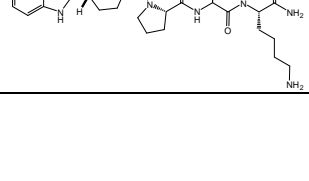

Table S2. HPLC data, MS data and chemical structures for the whole library of indoloquinolizidine-peptides.

Code	Chemical structure	t_R HPLC ₁ (min)	$M_{calc.}$	$M_{exp.}$ [M+H ⁺]
6{3,1,1}		5.93	657.4	658.4
6{4,1,1}		6.41	658.3	659.4
6{3,2,1}		6.79	680.4	681.5
6{4,2,1}		7.30	681.3	682.4
6{3,3,1}		6.89	677.4	678.5
6{4,3,1}		7.47	678.3	679.4
6{3,4,1}		6.73	659.4	660.4
6{4,4,1}		7.29	660.3	661.4
6{2,1,1}		6.36 6.64	657.4	658.4
6{2,2,1}		7.00 7.22	680.4	681.4

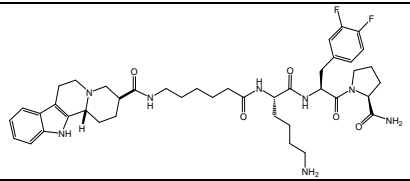
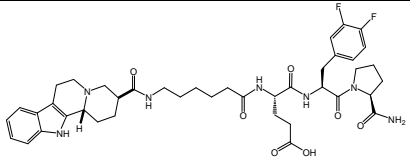
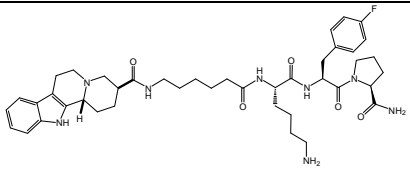
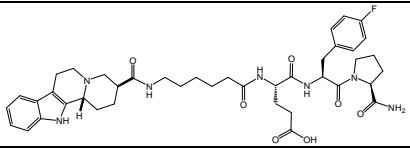
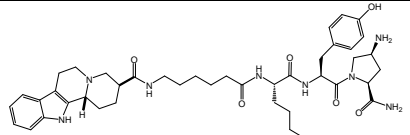
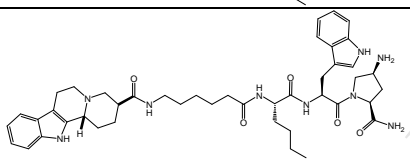
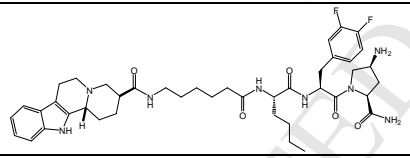
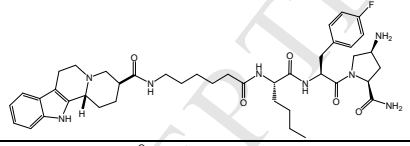
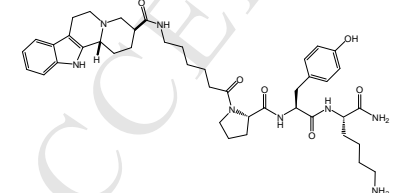
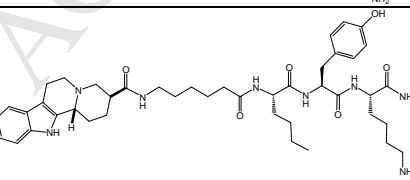
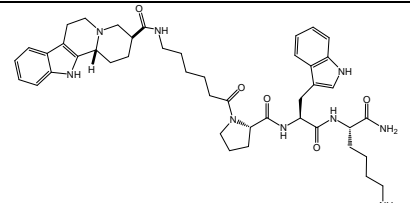
6{2,3,1}		7.20 7.43	677.4	678.4
6{2,4,1}		7.02 7.26	659.4	660.4
6{1,1,3}		5.54 5.82	657.4	658.5
6{2,1,3}		6.19 6.52	673.4	674.5
6{1,2,3}		6.34 6.59	680.4	681.5
6{2,2,3}		6.92 7.20	696.4	697.5
6{1,3,3}		6.65 6.85	677.4	678.4
6{2,3,3}		7.18 7.44	693.4	694.4
6{1,4,3}		6.46 6.66	659.4	660.4
6{2,4,3}		7.00 7.27	675.4	676.5
8{3,1,1}		6.12	770.5	771.5

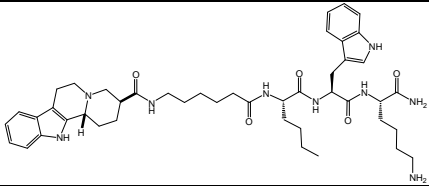
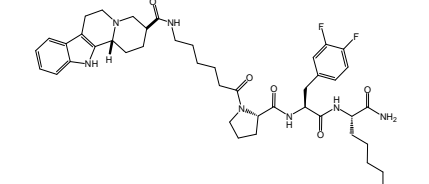
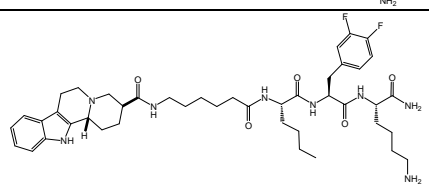
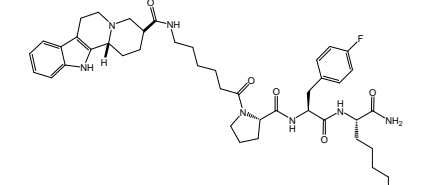
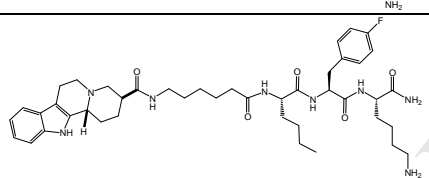
8{4,1,1}		6.62	771.4	772.5
8{3,2,1}		6.78	793.5	794.5
8{4,2,1}		7.39	794.4	795.5
8{3,3,1}		6.85	790.4	791.5
8{4,3,1}		7.51	791.4	792.5
8{3,4,1}		6.72	772.4	773.6
8{4,4,1}		7.33	773.4	774.5
8{2,1,1}		6.84	770.5	771.5
8{2,2,1}		7.40	793.5	794.6
8{2,3,1}		7.71	790.4	791.5
8{2,4,1}		7.52	772.4	773.5

8{1,1,3}		6.31	770.5	771.5
8{2,1,3}		6.84	786.5	787.5
8{1,2,3}		7.02	793.5	794.5
8{2,2,3}		7.47	809.5	810.5
8{1,3,3}		7.21	790.4	791.5
8{2,3,3}		7.77	806.5	807.5
8{1,4,3}		7.02	772.4	773.6
8{2,4,3}		7.59	788.5	789.5
7{3,1,1}		5.84	657.4	658.4
7{4,1,1}		6.33	658.3	659.4

7{3,2,1}		6.72	680.4	681.4
7{4,2,1}		7.23	681.3	682.4
7{3,3,1}		6.78	677.4	678.4
7{4,3,1}		7.38	678.3	679.4
7{3,4,1}		6.63	659.4	660.4
7{4,4,1}		7.15	660.3	661.4
7{2,1,1}		6.46 6.57	657.4	658.4
7{2,2,1}		7.01	680.4	681.4
7{2,3,1}		7.30 7.33	677.4	678.4
7{2,4,1}		7.11	659.4	660.4
7{1,1,3}		5.85	657.4	658.5

7{2,1,3}		6.43	673.4	674.5
7{1,2,3}		6.58 6.61	680.4	681.5
7{2,2,3}		7.13	696.4	697.5
7{1,3,3}		6.77	677.4	678.4
7{2,3,3}		7.40 7.44	693.4	694.4
7{1,4,3}		6.55	659.4	660.4
7{2,4,3}		7.17	675.4	676.5
9{3,1,1}		6.02	770.5	771.5
9{4,1,1}		6.43	771.4	772.5
9{3,2,1}		6.69	793.5	794.5
9{4,2,1}		7.19	794.4	795.5

9{3,3,1}		6.71	790.4	791.5
9{4,3,1}		7.26	791.4	792.4
9{3,4,1}		6.59	772.4	773.6
9{4,4,1}		7.16	773.4	774.4
9{2,1,1}		6.61	770.5	771.5
9{2,2,1}		6.15	793.5	794.5
9{2,3,1}		6.50	790.4	791.5
9{2,4,1}		7.23	772.4	773.5
9{1,1,3}		6.04	770.5	771.5
9{2,1,3}		6.65	786.5	787.5
9{1,2,3}		6.82	793.5	794.5

9{2,2,3}		7.30	809.5	810.5
9{1,3,3}		6.99	790.4	791.5
9{2,3,3}		7.62	806.5	807.5
9{1,4,3}		6.82	772.4	773.5
9{2,4,3}		7.36	788.5	789.5

3. High-throughput binding screening of the whole library at D₁R and D₂R.

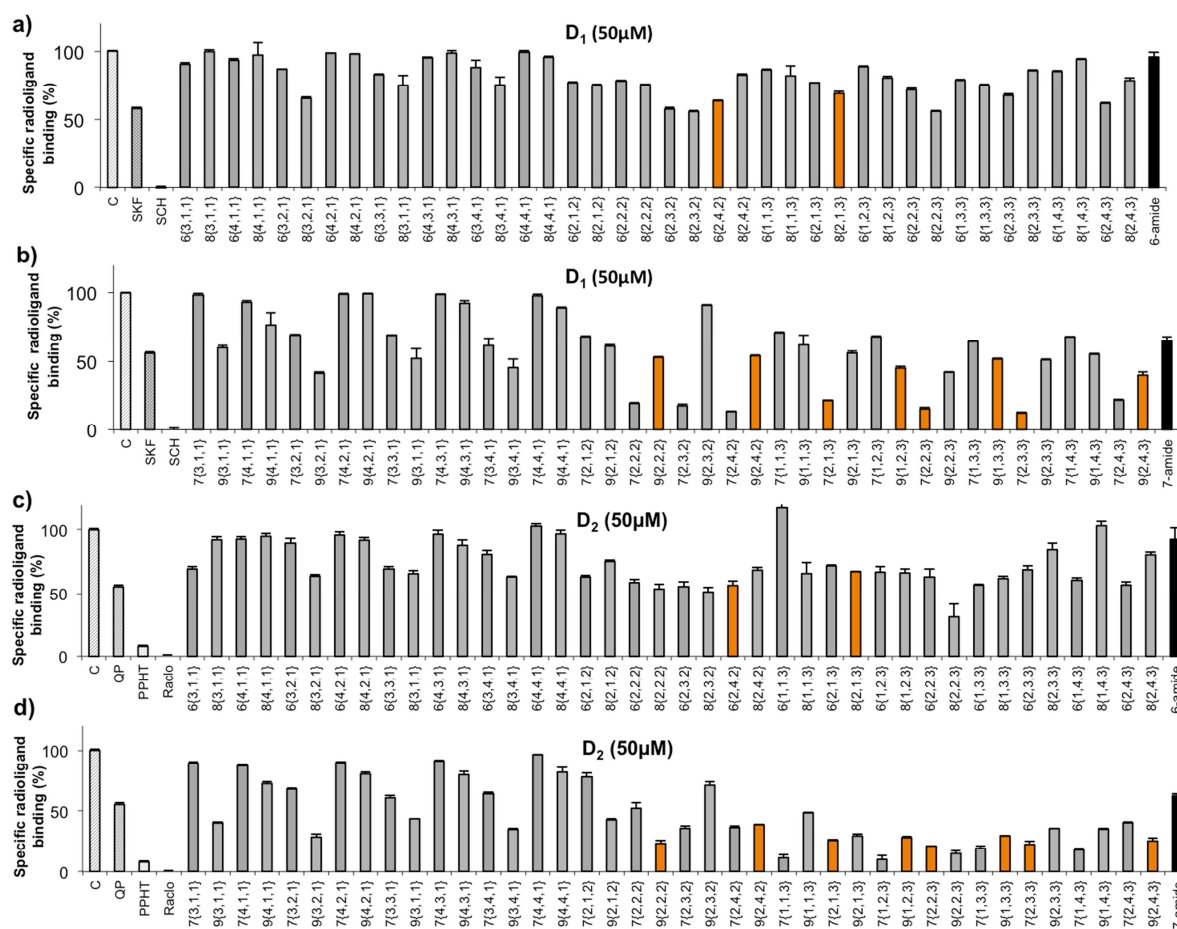


Figure S2. High-throughput binding screening of indoloquinolizidine-peptides at D₁R and D₂R. Specific binding at D₁R (a), (b) and D₂R (c), (d) as percentage of radioligand binding in the absence of competing ligand was measured as indicated in the Experimental Section. Highlighted in orange 10 compounds selected for the secondary screening. *Left bars:* control of radioligand binding without competing ligand; SKF & SCH: D₁R specific ligands; QP, PPHT & Raclo: D₂R specific ligands; others: radioligand specific binding in the presence of 50 μ M of the corresponding indoloquinolizidine-peptides. Radioligands used: a, b [³H]-SCH 23390, c, d [³H]-YM 09151-2. Data are represented as means \pm SD from a representative experiment ($n=3$) performed in triplicate. C: Control, PPHT: 2-(*N*-phenethyl-*N*-propyl)amino-5-hydroxytetralin, QP: quinpirole, Raclo: raclopride, SCH: SCH 23390; SKF: SKF-38393.

4. Screening of selected indoloquinolizidine-peptides at A₁ and A_{2A} adenosine receptors.**Table S3.** K_D (μM) values of selected indoloquinolizidine-peptides at A₁R and A_{2A}R.

	A₁R	A_{2A}R
6{2,4,2}	12±1	14±4
8{2,1,3}	> 100	16±2
9{1,2,3}	> 100	44±9
9{1,3,3}	> 100	37±5
7{2,1,3}	> 100	60±30
9{2,2,2}	> 100	18±3
7{2,2,3}	> 100	10±2
7{2,3,3}	> 100	26±3
9{2,4,2}	> 100	27±7
9{2,4,3}	> 100	11±2

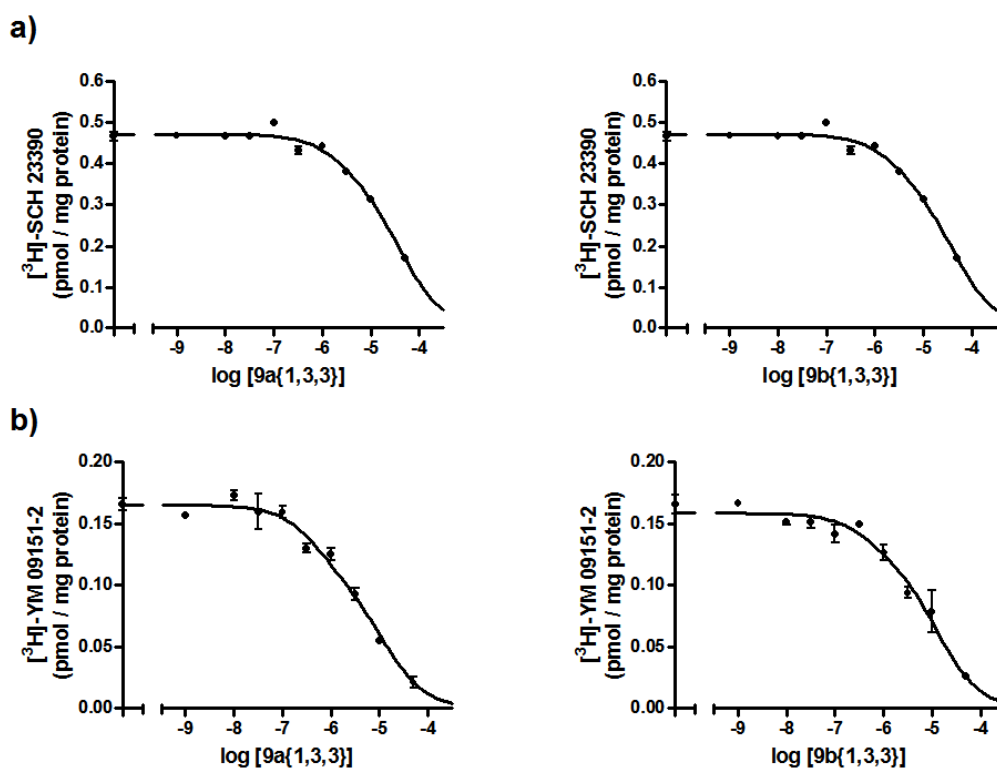
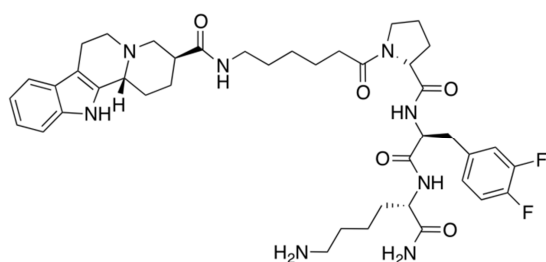
5. Binding curves for 9a{1,3,3} and 9b{1,3,3} at D₁R and D₂R.

Figure S3. Binding curves of 9a{1,3,3} and 9b{1,3,3} at D₁R (a) and D₂R (b). Competition between D₁R and D₂R antagonists (i.e. [³H]-SCH 23390 and [³H]-YM 09151-2 respectively) and increasing concentrations of 9a{1,3,3} and 9b{1,3,3} were performed in brain striatal membranes as indicated in the Experimental Section. Non-specific binding was determined in the presence of 50 μM SCH 23390 or 50 μM YM 09151-2. Data are represented as means ± SD from a representative experiment (*n* = 3) performed in triplicates.

6. Full characterisation data for 9a{1,3,3} and 9b{1,3,3}.

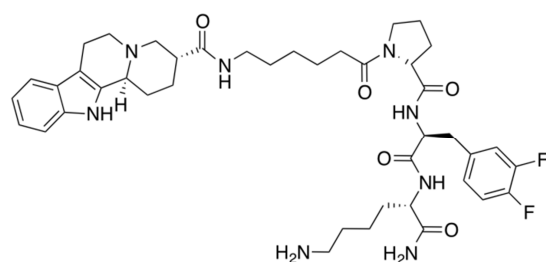


9a{1,3,3}: 17.2 mg, yellowish solid.

HRMS: (m/z) [M+H⁺] calcd. for C₄₂H₅₇F₂N₈O₅ 791.4420, found: 791.4384.

¹H-NMR (400 MHz, MeOD): 7.39 (d, *J*=8.0 Hz, 1H, Ar), 7.29 (d, *J*=8.0 Hz, 1H, Ar), 7.21-7.14 (m, 2H, Ar), 7.05 (t, *J*=6.8, 2H, Ar), 6.98 (t, *J*=9 Hz, 1H, Ar), 4.57-4.53 (m, 1H), 4.35-4.30 (m, 1H), 3.64-3.54 (m, 3H), 3.22-2.97 (m, 8H), 2.84-2.57 (m, 5H), 2.40 (t, *J*=8.4 Hz, 3H), 2.13-1.37 (m, 18H), 1.29 (bs, 1H), 1.21-0.98 (m, 1H)

¹³C-NMR (101 MHz, MeOD): 175.3, 175.0, 174.4, 173.7, 149.5, 136.9, 135.1, 127.6, 127.1, 125.7, 120.8, 120.8, 118.6, 118.1, 117.4, 117.0, 116.9, 110.6, 60.4, 60.2, 57.5, 54.8, 53.3, 53.2, 51.9, 43.2, 40.2, 38.9, 35.9, 34.0, 31.4, 29.4, 29.3, 29.0, 28.3, 27.6, 26.4, 24.5, 24.2, 22.8, 21.3.



9b{1,3,3}: 14.2 mg, yellowish solid.

HRMS: (m/z) [M+H⁺] calcd. for C₄₂H₅₇F₂N₈O₅ 791.4420, found: 791.4394.

¹H-NMR (400 MHz, MeOD): 7.38 (d, *J*=8.0 Hz, 1H, Ar), 7.28 (d, *J*=8.0 Hz, 1H, Ar), 7.19-7.15 (m, 2H, Ar), 7.04 (td, *J*=7.8, 1.2 Hz, 2H, Ar), 6.96 (td, *J*=7.8, 1.2 Hz, 1H, Ar), 4.67 (dd, *J*=10.2, 5.2 Hz, 1H), 4.54 (dd, *J*=8.6, 6.0 Hz, 1H), 4.35-4.28 (m, 2H), 3.67-3.53 (m, 2H), 3.22-2.86 (m, 7H), 2.77-2.56 (m, 5H), 2.38 (t, *J*=7.60 Hz, 2H), 2.14-1.39 (m, 19H), 1.29 (bs, 1H), 0.98-0.85 (m, 1H).

¹³C-NMR (101 MHz, MeOD): 176.2, 174.9, 174.9, 172.8, 138.1, 128.8, 128.3, 127.1, 126.9, 122.0, 119.8, 119.3, 119.2, 118.6, 118.2, 111.9, 110.4, 107.8, 61.6, 61.3, 58.7, 55.9, 54.5, 54.4, 44.4, 41.5, 41.3, 40.1, 37.1, 35.2, 32.6, 30.9, 30.5, 30.2, 29.4, 28.8, 27.6, 25.7, 25.3, 23.9, 22.4.